Contents

List of abbreviations

LCPR: Local cell production rate

REGR: Relative elementary growth rate

x: Distance from the quiescent center

dx/dt: Elongation rate

dx/dN: Length of the cortical cells

Ri: Inner radius of cortex

Ro: Outer radius of cortex

V: Cumulative cell volume

N: Cell number of cortical cell file

dV/dt: Volume growth rate

dV/dN: Cell volume

dN/dt: Cell production rate

FISH: Fluorescence *in situ* hybridization

WM-FISH: Whole-mount FISH

P: Cell proliferation zone

G1: Volume growth zone-1

G2: Volume growth zone-2

M: Mature zone

Preface

Polyploidy, the presence of three or more chromosomal sets in an organism, is widespread in land plants and is considered a driving force for speciation (Soltis et al., 2003; Jiao et al., 2011; Scarpino et al., 2014; Van de Peer et al., 2021). There are two types of polyploids: autopolyploids, whose chromosome sets come from the same species, and allopolyploids, derived from interspecific hybridization (Kihara and Ono, 1926). Historically, several researchers have believed that the majority of polyploid plants in nature are allopolyploids and that autopolyploids rarely exist in nature and are unlikely to contribute to speciation (ex., Stebbins, 1971; Grant, 1981). This historical bias led to the current research on allopolyploids being much broader and deeper than autopolyploids (Spoelhof et al., 2017). In recent decades, several researchers have proposed that autopolyploids are abundant in nature and are essential in the evolutionary context (Levin, 1983; Soltis et al., 2007, 2010; Barker et al., 2016; Spoelhof et al., 2017; Levin, 2019).

Here, I emphasize that it is important to analyze the effects of autopolyploidization on plant growth because it can also provide basis to analyze the effects of allopolyploidization. Allopolyploids, which have been mainly focused on the study of polyploids, are established through several pathways (Mason and Pires, 2015). Any formation pathway can be divided into two processes: hybridization and genome duplication (Soltis and Soltis, 2009). Autopolyploidization involves the latter of these two components alone, that is, genome duplication. Therefore, studying the effects of autopolyploidization can also be the first step in studying the effects of allopolyploidization.

Several previous studies have investigated the artificially generated autopolyploids of *Arabidopsis thaliana* to determine the effects of autopolyploidization on plants. The results of these studies reported that autopolyploidization of tetraploids promotes plant growth in several organs, such as flowers (Robinson et al., 2018), rosette leaves (Corneillie et al., 2019), and roots (Iwamoto et al., 2006). In such studies, tetraploids also exhibited larger and fewer cells than those of diploids (sepal cells, Robinson et al., 2018; pavement cells, Corneillie et al., 2019; cortical root cells, Iwamoto et al., 2006). Contrastingly, high-polyploids (e.g., hexaploids and octoploids) cause growth suppression called "high-ploidy syndrome" (Tsukaya, 2008). High-polyploids possess larger and fewer cells in an organ than those of diploids, similar to the tetraploids (Tsukaya, 2008; Robinson et al., 2018; Corneillie et al., 2019); however, they cause severe growth delay and dwarfed plant size compared to those of diploids and tetraploids (Kikuchi and Iwamoto, 2020). Nonetheless, it is still unclear what high-ploidy syndrome is and how it suppresses plant growth, although cell cycle delays might be involved (Comai, 2005). It remains undetermined whether cell proliferation and/or cell volume increase are repressed and where they are repressed in an organ of high-polyploids. Its mechanism remains to be elucidated.

In Chapter I of this thesis, I conducted a kinematic analysis of root growth on a cellular basis in the autoploid series of *A. thaliana* and determined the spatial profiles of growth parameters, such as cell proliferation rate and volume growth rate. This analysis aimed to clarify which growth parameters significantly influence the change in organ growth owing to autopolyploidization. Next, I conducted whole-mount fluorescence *in situ* hybridization (WM-FISH) analysis with a centromeric DNA probe on whole root tips of autopolyploids. The

analysis aimed to determine the spatial profile of the degree of chromosome polytenization in the root tips of autopolyploids, which may cause growth suppression by high-ploidy syndrome. Then, I compared the results of the WM-FISH analysis with those of the root growth analysis to elucidate the mechanism of the effects of autopolyploidization on root growth, including the high-ploidy syndrome.

In Chapter II, I focused on the effect of gelling agents on growth changes in roots owing to autopolyploidization in *A. thaliana*. Two gelling agents, agar and gellan gum, are considered to affect the change in root elongation owing to autopolyploidization. I aimed to demonstrate the differences and examine the physicochemical parameters gel hardness, water potential, and trace elements in each gelling agent to elucidate the key factors that caused these differences. The results shed light on the influence of environmental factors on growth change caused by autopolyploidization.

References

Barker MS, Arrigo N, Baniaga AE, Li Z, Levin DA (2016) On the relative abundance of autopolyploids and allopolyploids. *New Phytologist* **210**:391–398. https://doi.org/10.1111/nph.13698

Comai L (2005) The advantages and disadvantages of being polyploid. *Nature Reviews Genetics* **6**:836–846. https://doi.org/10.1038/nrg1711

Corneillie S, De Storme N, Van Acker R, Fangel JU, De Bruyne M, De Rycke R, Willats WGT, Vanholme B, Boerjan W (2019) Polyploidy Affects Plant Growth and Alters Cell Wall Composition. *Plant Physiology* **179**:74–87. https://doi.org/10.1104/pp.18.00967

Grant V (1981) Plant Speciation. *Columbia University Press*. https://doi.org/10.7312/gran92318

Iwamoto A, Satoh D, Furutani M, Maruyama S, Ohba H, Sugiyama M (2006) Insight into the basis of root growth in *Arabidopsis thaliana* provided by a simple mathematical model. *Journal of Plant Research* **119**:85–93. https://doi.org/10.1007/s10265-005-0247-x

Jiao Y, Wickett NJ, Ayyampalayam S, Chanderbali AS, Landherr L, Ralph PE, Tomsho LP, Hu Y, Liang H, Soltis PS (2011) Ancestral polyploidy in seed plants and angiosperms. *Nature* **473**:97. https://doi.org/10.1038/nature09916

Kihara H, Ono T (1926) Chromosomenzahlen und systematische Gruppierung der Rumex-Arten. *Zeitschrift für Zellforschung und Mikroskopische Anatomie* **4**:475–481. https://doi.org/10.1007/BF00391215

Kikuchi S, Iwamoto A (2020) Quantitative analysis of chromosome polytenization in synthetic autopolyploids of *Arabidopsis thaliana*. *Cytologia* **85**:189–195. https://doi.org/10.1508/cytologia.85.189

Levin DA (1983) Polyploidy and novelty in flowering Plants. *The American Naturalist* **122**:1–25. https://doi.org/10.1086/284115

Levin DA (2019) Plant speciation in the age of climate change. *Annals of Botany* **124**:769–775. https://doi.org/10.1093/aob/mcz108

Mason AS, Pires JC (2015) Unreduced gametes: meiotic mishap or evolutionary mechanism? *Trends in Genetics* **31**:5–10. https://doi.org/10.1016/j.tig.2014.09.011

Robinson DO, Coate JE, Singh A, Hong L, Bush M, Doyle JJ, Roeder AHK (2018) Ploidy and size at multiple scales in the Arabidopsis sepal. *The Plant Cell* **30**:2308–2329. https://doi.org/10.1105/tpc.18.00344

Scarpino SV, Levin DA, Meyers LA (2014) Polyploid formation shapes flowering plant diversity. *The American Naturalist* **184**:456–465. https://doi.org/10.1086/677752

Soltis DE, Buggs RJA, Doyle JJ, Soltis PS (2010) What we still don't know about polyploidy. *Taxon* **59**:1387–1403. https://doi.org/10.1002/tax.595006

Soltis DE, Soltis PS, Schemske DW, Hancock JF, Thompson JN, Husband BC, Judd WS (2007) Autopolyploidy in angiosperms: have we grossly underestimated the number of species? *Taxon* **56**:13–30. https://doi.org/10.2307/25065732

Soltis DE, Soltis PS, Tate JA (2003) Advances in the study of polyploidy since plant speciation. *New Phytologist* **161**:173–191. https://doi.org/10.1046/j.1469-8137.2003.00948.x

Soltis PS, Soltis DE (2009) The role of hybridization in plant speciation. *Annual Review of Plant Biology* **60**:561–588. https://doi.org/10.1146/annurev.arplant.043008.092039

Spoelhof JP, Soltis PS, Soltis DE (2017) Pure polyploidy: closing the gaps in autopolyploid research. *Journal of Systematics and Evolution* **55**:340–352. https://doi.org/10.1111/jse.12253

Stebbins GL (1971) Chromosomal evolution in higher plant. *Edward Arnold, London.*

Tsukaya H (2008) Controlling size in multicellular organs: focus on the leaf. *PLoS Biology* **6**:e174. https://doi.org/10.1371/journal.pbio.0060174

Van de Peer Y, Ashman TL, Soltis PS, Soltis DE (2021) Polyploidy: an evolutionary and ecological force in stressful times. *The Plant Cell* **33**:11–26. https://doi.org/10.1093/plcell/koaa015

Quantitative analysis of the effects of the progression of autopolyploidization on cell proliferation, cell volume increase, and chromosome behavior in *Arabidopsis thaliana*

Abstract

I conducted a kinematic analysis of the root tip cells in *Arabidopsis thaliana* autopolyploids (diploid, tetraploid, hexaploid, and octoploid) to characterize the effects of genome duplication on root growth. The results of the root growth analysis showed that tetraploidization promotes cell volume increase, but suppresses cell proliferation. The polyploidization leading to the development of high-polyploids (hexaploids or octoploids) suppresses cell proliferation, but also cell volume increase in the volume growth and mature zones of the root. I subsequently established a new whole-mount fluorescence *in situ* hybridization (WM-FISH) method for analyzing the whole *A. thaliana* root in terms of the spatial profile of the number of centromere signals associated with chromosome polytenization. The WM-FISH analysis revealed that endoreduplication was suppressed in the high-polyploids and chromosome polytenization was extensive in the volume growth and mature zones, in which the cell volume increase were significantly suppressed (relative to the corresponding values in the diploids and tetraploids). The results of the kinematic analysis and the WM-FISH analysis suggest the importance of chromosome polytenization for the suppressed growth in high-polyploids (i.e., high-ploidy syndrome). The study findings provide crucial insights into the mechanisms underlying the changes in plant organ growth associated with autopolyploidization, particularly in high-polyploids.

Introduction

The root is a good model for analyzing plant organ growth because it has a relatively simple structure (Dolan et al., 1993) and grows almost one-dimensionally (Erickson, 1976) with spatially divided growth zones (i.e., cell proliferation, transition, elongation, and mature zones) (Verbelen et al., 2006). In previous studies, kinematic analyses of *Arabidopsis thaliana* root tip cells were performed to quantitatively elucidate the spatial profile of specific growth parameters (Beemster and Baskin, 1998; West et al., 2004; Iwamoto et al., 2006). For example, Iwamoto et al. (2006) characterized the root growth parameters of autotetraploid and diploid *A. thaliana*, and showed that the autopolyploidization resulting in tetraploids leads to an increase in the cell volume and the suppression of cell proliferation. I extended this analysis to the root growth of high-polyploids.

In the study described in this chapter, I established a series of *A. thaliana* autopolyploids, including high-polyploids (e.g., hexaploid and octoploid), and performed a kinematic analysis of cells to determine the effect of the progression of autopolyploidization on the spatial profile of individual root growth parameters. The results of the root growth analysis revealed which changes in growth parameters positively and negatively affect organ growth in autopolyploid plants.

Autopolyploids have been studied to precisely characterize the growth changes due to autopolyploidization as well as the underlying mechanism. The altered growth of autopolyploids is caused by the changes to transcript levels associated with genome duplication events. Song et al. (2020) reported that the total transcript abundance increased in autotetraploid *A. thaliana*, but it was less

than double that of its diploid ancestors, suggesting that autopolyploidization may increase gene expression, but the increase is not proportional to the genome size. In general, chromosome structural changes are associated with changes in gene expression (Jarillo et al., 2009; Song et al., 2021). Therefore, autopolyploidization-induced modifications to chromosome structures may modulate gene expression, which should be considered when examining the mechanism underlying the growth changes due to autopolyploidization. Chromosome polytenization in the leaf cells of *A. thaliana* autopolyploids (Breuer et al., 2007; Kikuchi and Iwamoto 2020) was confirmed via a fluorescence *in situ* hybridization (FISH) analysis involving a centromeric DNA probe. The chromosome polytenization in autopolyploids could affect gene expression as well as cell proliferation because it influences chromosome segregation.

In this study, I used a centromeric DNA probe to perform a whole-mount FISH (WM-FISH) analysis of the whole root tips of autopolyploids. The aim of this study was to clarify the spatial profile of the degree of chromosome polytenization in the root tips of *A. thaliana* autopolyploids. I subsequently compared the results of the WM-FISH analysis with the results of a root growth analysis to elucidate the relationship between growth traits and chromosome dynamics. The study results provide insights into the mechanisms mediating the growth changes due to the progression of autopolyploidization (e.g., high-ploidy syndrome) (Tsukaya, 2008).

Materials and Methods

Production of synthetic *Arabidopsis thaliana* autopolyploids

Synthetic *A. thaliana* (L.) Heynh. autopolyploids (tetraploid, hexaploid, and octoploid) were produced by treating diploid seedlings with colchicine (Kikuchi and Iwamoto 2021). The ploidy level was determined by a flow cytometry analysis. The ploidy level of the generated autopolyploid strains was confirmed for at least three generations after the colchicine treatment before the autopolyploids were used for the kinematic analysis.

Flow cytometry analysis

Leaf samples for the flow cytometry analysis were collected from seedlings at 30–40 days after sowing (DAS). The ploidy level of each strain was verified using a flow cytometer (CyFlow Ploidy Analyzer PA, Sysmex Partec GmbH, Münster, Germany) and the previously described chopping method (Johnston et al. 1999).

Plant materials and growth conditions

The seeds of *A. thaliana* (ecotype Columbia) autopolyploids (diploid, tetraploid, hexaploid, and octoploid) were surface-sterilized in a 20% sodium hypochlorite solution containing 0.5% Triton X-100. The seeds were sown in each growth medium in plates, which were then incubated in a vertical position for 10 days under constant conditions (22 °C and continuous light at 90 μmol m^{-2} s^{-1}). The growth media used in this study contained the following common components (per liter): 10 g sucrose, 0.5 g 2-morpholinoethanesulfonic acid, 10 mL Murashige and Skoog (MS) vitamins (10.0 mg/L thiamine, 0.5 mg/L pyridoxine,

0.5 mg/L nicotinic acid, and 100 mg/L inositol), and 2.3 g MS Plant Salt Mixture (Wako Pure Chemical Industries, Osaka, Japan). The solid media contained 0.8% (w/v) gellan gum (Lot #SLBV6512, G1910-250G; Sigma Life Science, St. Louis, MO, USA).

Measurement of the root elongation rate

Te initial position of the root tip was marked on the plate to determine the root elongation rate for each seedling. The measurement was conducted from 5 DAS to 10 DAS and the marked plate was digitally scanned. The distance between successive marks along the roots in the digitized images was measured using ImageJ (version 1.51m9) (Rasband, W.S., ImageJ, U. S. National Institutes of Health, Bethesda, Maryland, USA, https://imagej.nih.gov/ij/, 1997-2018). The average root elongation rate (per hour) was calculated for each measurement date by dividing the measured distance of the root tip movement by the corresponding time interval between markings (approximately 24 h).

Kinematic analysis of cells

Measurement of the elongation rate

The 3 mm apical portion of the *A. thaliana* primary roots was photographed using a video microscope (VHX6000, Keyence, Osaka, Japan) at 8 DAS (Fig. I-1). The same roots were photographed 30 min later under the same conditions. The Neo Measure (Iwamoto et al., in prep; LPixel, Tokyo, Japan) was used to examine the two images and measure the displacement rate of each point of the root tip. By

determining the same point in the two images and measuring the distance between these points, the elongation rate (*dx/dt*) at various points of the root tip was calculated (Fig. I-2).

Measurement of the cell length

After the elongation rate was determined, the roots were cut at approximately 3 mm from the tip and fixed in 90% acetone for 1 h. The fixed root tips were washed with 0.1 mM phosphate buffer (pH 7.0) and mounted on glass slides with 50% glycerol. The samples were examined using the Nomarski differential interference contrast microscope (BX50, Olympus, Tokyo, Japan) and the cortical cell files in the region approximately 400–3,000 μm from the quiescent center (QC) were photographed. The same root tips were immersed in transparency solution (4 g chloral hydrate, 1 mL glycerin, and 2 mL deionized water) for at least 24 h, after which the region approximately 400 μm from the QC was photographed. Using the captured images, the length of the cortical cells (*dx/dN*) and the inner and outer radii (*Ri* and *Ro*) of the cortical cell files at each point of the root tip were measured using the Root Cell Size Measurer (in Ij Tool, LPixel, Tokyo, Japan). Root Cell Size Measurer is a plugin of ImageJ that semi-automatically measures the *dx/dN*, *Ri*, and *Ro* of the cortical cell files using a manually traced image of the cortical cells. This program enabled the semi-automatic measurement of each cortical cell growth parameter in the region 3 mm from the QC (Fig. I-3).

Conversion of the elongation rate and cell length to cell volume: calculation of the cell volume and growth rate

In *A. thaliana*, root thickness varies among ploidy levels (Fig. I-5a–c). Therefore, a volume-based analysis is required to obtain an accurate spatial growth pattern. Because the *A. thaliana* root cortical layer comprises eight rows of cells and the entire root tip can be considered as a rotating body, the distance-based data were converted to volume-based data (Iwamoto et al., 2006). The cross-sectional area (S) of one cortical cell file at a distance x from the QC was calculated using the following equation:

$$S(x) = \frac{\pi}{8}\left[\{Ro(x)\}^2 - \{Ri(x)\}^2\right] \quad (1)$$

By integrating S from 0 (the QC) to distance x, the volume (V) of the cortical cell file at a distance x from the QC was determined using the following equation:

$$V(x) = \int_0^x S(x)dx \quad (2)$$

Using the above method, dx/dt and dx/dN were converted to volume-based data and the rate of the volume increase (dV/dt) and cell volume (dV/dN) in the cortical cell file for various cumulative volumes (V) from the QC were calculated.

Because the data for each root tip were discrete, they were smoothed twice using the super smoother method (Friedman 1984). Additionally, the data points were connected using a spline function to form a function for the cell volume (V). This function was used in the subsequent analyses.

$$\frac{dN}{dt} = \frac{dN}{dV} \times \frac{dV}{dt} \tag{3}$$

The number of cells (N) was obtained by integrating dN/dV and V.

$$N = \int_0^V \frac{dN}{dV} dV \tag{4}$$

The relative elementary growth rate (REGR) is derived from the volume growth rate (dV/dt) divided by the volume (V) and was determined using the following equation:

$$\text{REGR} = \frac{d\left(\frac{dN}{dt}\right)}{dV} \tag{5}$$

The REGR represents the relative rate of the cell volume increase at a given position in the root. The volume growth zone corresponds to the region from the QC to the position where REGR decreases to 0.

The local cell production rate (LCPR) is derived from the cell proliferation rate (dN/dt) divided by the volume (V) and was calculated using the following equation:

$$\text{LCPR} = \frac{d\left(\frac{dV}{dt}\right)}{dV} \tag{6}$$

The LCPR represents the local (not cumulative) number of cells produced per unit time at any given location in the root. The cell proliferation zone refers to the region from the QC to the position where LCPR decreases to 0.

Numerical calculations

The R program (R for Mac OS 4.0.3, R Development Core Team, 2020) was used for calculating each parameter.

Whole-mount fluorescence *in situ* hybridization analysis

Probe preparation

A PCR system was used to amplify probe fragments. The reactions were completed in a final volume of 50 μL containing 5 μL each primer (ATH180F: 5′-GATCAAGTCATATTCGACTC-3′; ATH180R: 5′-GTTGTCATGTGTATGATTGA-3′, 10 μM each), 5 μL 10× Ex Taq buffer (Takara, Shiga, Japan), 5 μL 0.3 mM d(A, G, T)TP, 1 μL 0.1 mM dCTP, 1 μL 50 ng/μL *A. thaliana* genomic DNA, 25 μL Milli-Q water, 2.5 μL Cy3-dCTP (Cytiva, Tokyo, Japan), and 0.5 μL Taq DNA polymerase (5 U/μL; Takara). The PCR amplification was performed using a thermal cycler (Thermal Cycler Dice Touch; Takara) and the following program: 96 °C for 1 min; 30 cycles of 96 °C for 45 s, 50 °C for 45 s, and 45 °C for 1 min; and 72 °C for 10 min. Prior to the WM-FISH analysis, labeled probes were precipitated and resuspended in SF50 (2× SSC and 50% formamide, pH 7; SSC: 0.3 M sodium citrate and 3M NaCl, pH 7.0).

Preservation of the whole root shape

I used silicon wells that were developed for culturing cells on glass slides to perform the WM-FISH analysis, during which the shape of the whole root tip was preserved. First, fixed root samples were adhered to MAS-coated glass slides. Next, silicon wells were attached to the glass slides to surround the root samples. The silicon wells functioned as walls surrounding the root samples on the glass slides during the immersion of the roots in each reagent. Because the initial processing steps were performed on glass slides instead of in tubes or bottles, the root samples were prevented from floating. Floating roots during the FISH procedure (e.g., enzyme treatment) tend to become twisted or tangled, which can severely damage the root tissues, and the roots may break when the samples are transferred to glass slides after the hybridization. I carefully removed the silicon wells, placed vinyl tape around the root tips, and mounted the samples in Vectashield (Vector Laboratories, Peterborough, UK) containing 1.5 mg/mL 4′,6-diamidino-2-phenylindole (DAPI). This technique is more efficient than conventional FISH techniques using tubes or bottles because it requires less reagent (150–300 μL) to immerse each root sample.

Hybridization

The hybridization was completed according to a modified version of the method developed by Berr and Schubert (2007). Root tips (approximately 1 cm) excised from seedlings at 8 DAS were fixed in 4% formaldehyde in phosphate-buffered saline (PBS; 50 mM NaH_2PO_4 and 150 mM NaCl, pH 7.4) for 20 min and then washed with PBS (twice for 5 min each). The roots were carefully placed on MAS-coated glass slides (MAS-GP type A, Matsunami Glass, Osaka, Japan) and silicon wells (3-well chamber, removable, Ibidi, Gräfeling, Germany) were attached to the slides.

In the following procedure, unless otherwise stated, 300 μL reagent was carefully added to each well, followed by an incubation in methanol (twice for 5 min each) and 99.5% ethanol (twice for 5 min each) and a rehydration in PBS (twice for 10 min each). The roots were rinsed in distilled water (twice for 5 min each) and citrate buffer (10 mM sodium citrate, pH 4.8; twice for 5 min each) and digested with 2% (w/v) Cellulase (R-10, Yakult Pharmaceutical, Tokyo, Japan) and 0.5% (w/v) Pectolyase (Y-23, Kyowa Chemical Products, Osaka, Japan) in citrate buffer at 37 °C for 45 s.

The duration of the enzyme treatment depends on the sample. If the duration of the enzyme treatment is too short, the probe will not be able to enter the cells, resulting in a lack of hybridization. Conversely, if the duration of the enzyme treatment is too long, the cell wall will be over-digested and brittle, thereby increasing the possibility that the root will be misshapen. Roots often break in the region slightly above the edge of the lateral root cap, which is assumed to be the elongation zone. The reorganization of cell wall components and cell wall loosening in the elongation zone have been reported (Wolf et al., 2011; Somssich et al., 2016). Previous studies revealed that the root mechanical strength is lower in the volume growth region than in the meristematic region (Kozlova et al., 2019; Samalova et al., 2020), suggesting that the cell walls in the volume growth zone are fragile. Thus, it is important to minimize the duration of the enzyme treatment for the WM-FISH analysis to preserve the root shape. The results of my preliminary experiments indicated that a 45 s enzyme treatment was optimal for WM-FISH because the shape of the whole root tip of *A. thaliana* was unaffected.

After the enzyme treatment, the roots were immediately washed in PBS (twice for 10 min each), postfixed in 4% formaldehyde in PBS (20 min), and

prehybridized in SF50 for 1 h at 50 °C. Probes were denatured together with the root samples in 150 μL (per well) hybridization solution for 4 min at 96 °C. Samples were placed on an ice block for 5 min prior to the hybridization at 37 °C for more than 40 h. To prevent samples from drying or being exposed to light, the silicon wells were covered with plastic wrap and aluminum foil. Following the hybridization, the roots were washed with 2× SSC, 1× SSC, and distilled water at 37 °C for 15 min each. They were then mounted in Vectashield (Vector Laboratories, Burlingame, CA, USA) containing 1.5 mg/mL DAPI and covered with a cover glass. Vinyl tape was applied to distribute the weight of the cover glass to avoid crushing the roots.

Microscopy, image processing, and data analysis

Images of the Z-serial optical sections (Fig. I-4a, b) were captured using a confocal laser scanning microscope (FV1000-D, Olympus, Tokyo, Japan). The obtained confocal images were converted to 3D images (Fig. I-4c, d) using the Amira software (version 2019.4, Mercury Computer Systems, Berlin, Germany). Cortical cell files in the 3D images were identified using differential interference contrast images. The nuclear volume and the number of centromere signals at each root position were calculated using the Label Analysis module in Amira. Fused nuclei due to aggregation were not used for calculating the nuclear volume and the number of centromere signals because the nuclear volume could not be calculated accurately.

Results

Analysis of autotetraploid *Arabidopsis thaliana* root growth

I examined root growth by performing a kinematic analysis of cells to elucidate the effects of autotetraploidization on *A. thaliana* root growth (Fig. I-5a, d, g, j, m; Fig. I-6a, d; Fig. I-7a, d). The calculated parameters were plotted versus the distance (μm) from the QC or the number of cells in the cortical cell files from the QC. The following sections describe the differences in the spatial patterns of each growth parameter between the tetraploids and the diploids.

Cumulative cell volume (*V*)

The cumulative cell volume is a growth parameter that reflects the root thickness (i.e., an increase in the cumulative cell volume indicates an increase in root thickness). The cumulative cell volume in the whole root region was greater for the tetraploids than for the diploids. I compared the growth parameter of the tetraploids with that of the diploids at every 25 μm from the QC to 2,800 μm; minimum 1.15-times and maximum 1.27-times larger for tetraploid-1 and minimum 1.22- times and maximum 1.35-times larger for tetraploid-2 (Fig. I-5a).

Volume growth rate (*dV/dt*)

The tetraploids (tetraploid-1 and tetraploid-2) and diploids had similar spatial patterns in the volume growth rate (Fig. I-5d). Although tetraploid-1 had almost the same volume growth rate as the diploid, tetraploid-2 had a slightly higher volume growth rate than the diploid. As with the results of Cumulative cell volume, I compared the growth parameter of the tetraploids with that of the diploids at every 25 μm from the QC to 2,800 μm; minimum 1.00-times and maximum 1.04-times larger for tetraploid-1 and minimum 1.11- times and maximum 1.16-times larger for tetraploid-2 (Fig. I-5d). The volume growth rates

at 2,800 μm from the QC (i.e., steady-state root growth) were 5.29×10^5 μm^3 h^{-1} (diploid), 5.43×10^5 μm^3 h^{-1} (tetraploid-1), and 6.08×10^5 μm^3 h^{-1} (tetraploid-2).

Cell volume (*dV/dN*)

Although the spatial patterns in the cell volume were similar between the tetraploids and diploids, the cell volume increased significantly more for the tetraploids than for the diploids. Comparing the growth parameters of the tetraploids with those of the diploids at every 25 μm from the QC to 2,800 μm, the cell volume were 1.18- to 1.26- times larger for tetraploid-1 and 1.27- to 1.39-times larger for tetraploid-2 than for diploid (Figure I-5g).

Cell production rate (*dN/dt*)

The cell production rate was slightly lower for the tetraploids than for the diploids (Fig. I-5j). The cell production rates at 2,800 μm from the QC (i.e., steady-state root growth) were 2.46 cell h^{-1} (diploid), 2.08 cell h^{-1} (tetraploid-1), and 2.10 cell h^{-1} (tetraploid-2).

Cell number (*N*)

Tetraploid-1 and tetraploid-2 had a similar number of cells (Fig. I-5m), but the cell number in the region from 25 μm to 2,800 μm from the QC was 0.84- to 0.92-times lower in tetraploids than in diploids (Figure I-5m).

Relative elementary growth rate (REGR)

The spatial pattern of the REGR was calculated using the volume growth rate (Fig. I-6a; see Materials and Methods). The REGR represents the relative rate of

the cell volume increase at any given point along the root. The volume growth zone corresponds to the region from the QC to where REGR decreases to 0.

In tetraploid-1, REGR peaked at 725 μm from the QC, whereas in tetraploid-2 and the diploids, it peaked at 825 μm from the QC. The peak REGR was slightly lower for the tetraploids (tetraploid-1, 4.19×10^{-1} h^{-1}; tetraploid-2, 4.00×10^{-1} h^{-1}) than for the diploids (4.29×10^{-1} h^{-1}).

The REGR decreased to 0 at 2,650–2,675 μm (diploid), 2,600–2,625 μm (tetraploid-1), and >3,000 μm (tetraploid-2) from the QC. These results indicate that the polyploidization resulting in tetraploids did not lead to the expansion of the volume growth zone.

Local cell production rate (LCPR)

The spatial pattern of the LCPR was calculated using the cell production rate (Fig. I-6d; see Materials and Methods). The LCPR represents the number of cells produced locally at a given point in the root. The cell proliferation zone corresponded to the region from the QC to where LCPR decreased to 0.

In the region near the QC (<200 μm from the QC), the LCPR was lower for the tetraploids than for the diploids, indicative of suppressed cell proliferation (Fig. I-6d inset). However, the distance between the QC and the point at which LCPR decreased to 0 was almost the same for the tetraploids (325–350 μm) and the diploid (350–375 μm), implying there was no significant difference in the size of the cell proliferation zone between the tetraploids and diploids.

I also plotted the cell production rate versus the number of cortical cells from the QC (Fig. I-7a) and calculated the LCPR (Fig. I-7d). The number of cortical cells in the cell proliferation zone decreased following tetraploidization

(Fig. I-7d). Specifically, the cell number in the cell proliferation zone was 57 for the diploid and 49 for tetraploid-1 and 46 for tetraploid-2.

Analysis of *A. thaliana* autohexaploids and autooctoploids in terms of their root growth

I performed a kinematic-based analysis of the root growth of the *A. thaliana* hexaploids and octoploids (Fig. I-5b, c, e, f, h, i, k, l, n, o; Fig. I-6b, c, e, f; Fig. I-7b, c, e, f). Similar to the data for the diploids and tetraploids, the calculated parameters were plotted versus the distance from the QC (μm) or the number of cells in the cortical cell files from the QC.

Cumulative cell volume (*V*)

The cumulative cell volumes in the whole root region were greater for the hexaploids and octoploids than for the diploids. I compared the growth parameter of the hexaploids and octoploids with that of the diploids at every 25 μm from the QC to 2,800 μm; minimum 1.26-times and maximum 1.37-times larger for hexaploid-1, minimum 1.18-times and maximum 1.28-times larger for tetraploid-2, minimum 1.21-times and maximum 1.53-times larger for octoploid-1, minimum 1.15-times and maximum 1.37-times larger for octoploid-2 (Fig. I-5a). Cumulative cell volume of high-polyploids was almost the same or smaller than that of tetraploids, indicating that the increase in root thickness was not proportional to the ploidy level (Fig. I-5a–c).

Volume growth rate (*dV/dt*)

The volume growth rate in the apical region from the QC to approximately 900 μm was greater for the hexaploids than for the diploids; there was no significant increase in the subsequent region (Fig. I-5e). The volume growth rates at 2,800 μm from the QC (steady-state root growth) were lower in the hexaploids than in the diploids (0.50-times lower for hexaploid-1 and 0.52-times lower for hexaploid-2).

The volume growth rate in the region from the QC to approximately 800 μm was greater for the octoploids than for the diploids and hexaploids; there was almost no increase in the subsequent region (Fig. I-5f). The volume growth rates at 2,800 μm from the QC (steady-state root growth) were lower in the octoploids than in the diploids and hexaploids (0.30-times lower for octoploid-1 and 0.41-times lower for octoploid-2).

The volume growth rates at the point where the root growth reached a steady state (2,800 μm from the QC) were 5.24×10^5 μm^3 h^{-1} (diploid), 2.65×10^5 μm^3 h^{-1} (hexaploid-1), 2.76×10^5 μm^3 h^{-1} (hexaploid-2), 1.60×10^5 μm^3 h^{-1} (octoploid-1), and 2.17×10^5 μm^3 h^{-1} (octoploid-2).

Cell volume (*dV/dN*)

The cell volumes in the region near the QC were greater for the hexaploids and octoploids than for the diploids (Fig. I-5h, i). The hexaploids and the diploid had a similar spatial pattern, with the cell volume continuing to increase slightly in the region >2,000 μm from the QC (Fig. I-5h). In contrast, for the octoploids, the cell volume almost stopped increasing in the region >1,500 μm from the QC (Fig. I-5i). The cell volumes at 2,800 μm from the QC (steady-state root growth) were 1.85×10^5 μm^3 (hexaploid-1), 1.87×10^5 μm^3 (hexaploid-2), 1.39×10^5 μm^3 (octoploid-1), and 1.67×10^5 μm^3 (octoploid-2).

Cell production rate (*dN/dt*)

The cell production rates were lower for the hexaploids and octoploids than for the diploids (Fig. I-5k, l). Notably, the cell production rate was significantly suppressed in the octoploids. The cell production rates at 2,800 μm from the QC (steady-state root growth) were 2.46 cell h^{-1} (diploid), 1.72 cell h^{-1} (hexaploid-1), 1.53 cell h^{-1} (hexaploid-2), 1.23 cell h^{-1} (octoploid-1), and 1.35 cell h^{-1} (octoploid-2).

Cell number (*N*)

Compared with the cell number of the diploids and tetraploids, the cell number decreased significantly in the hexaploids (Fig. I-5m, n) and decreased even more in the octoploids (Fig. I-5m, o), indicating that the cell number decreases as polyploidization progresses. The cell numbers in the region from 25 μm to 2,800 μm from the QC were almost the same in strains having the same ploidy levels and 0.75- to 0.85-times lower for hexaploids and 0.62- to 0.81-times lower for octoploids than for diploids.

Relative elementary growth rate (REGR)

The spatial pattern of the REGR was calculated using the volume growth rate (Fig. I-6b, c). The REGR peaked closer to the QC in the hexaploids and octoploids than in the diploids. The REGR peaked at 700 μm (from the QC) in hexaploid-1, 625 μm in hexaploid-2, and 575 μm in octoploid-1 and octoploid-2. The REGR peak of the high-polyploids was significantly lower than that of the diploids and tetraploids (hexaploid-1, 3.33×10^{-1} h^{-1}; hexaploid-2, 3.46×10^{-1} h^{-1}; octoploid-1, 2.86×10^{-1} h^{-1}; octoploid-2, 3.01×10^{-1} h^{-1}). The distances

from the QC to the point at which the REGR was 0 for the high-polyploids were 1,850–1,875 μm (hexaploid-1), 2,400–2,425 μm (hexaploid-2), 2,000–2,025 μm (octoploid-1), and 1,450–1,475 μm (octoploid-2). Thus, the volume growth zone was smaller for the hexaploids and octoploids than for the diploids and tetraploids.

Local cell production rate (LCPR)

The spatial pattern of the LCPR was then calculated using the cell production rate (Fig. I-6e, f; see Materials and Methods). The LCPR in the region near the QC (<200 μm from the QC) was significantly lower for the hexaploids and octoploids than for the diploids, suggesting that cell proliferation was significantly suppressed in the high-polyploids. The distances from the QC to the point at which the LCPR decreased to 0 (i.e., the end of the cell proliferation zone) were 350–375 μm (diploid), 275–300 μm (hexaploid-1), 300–325 μm (hexaploid-2), 275–300 μm (octoploid-1), and 250–275 μm (octoploid-2). Accordingly, the size of the cell proliferation zone decreased slightly in the high-polyploids.

Next, I plotted the cell production rate versus the number of cortical cells from the QC (Fig. I-7b, c) and calculated the LCPR (Fig. I-7e, f). There were fewer cortical cells in the cell proliferation zone in the high-polyploids (especially the octoploids) than in the diploids and tetraploids, reflecting the decrease in cell proliferation as polyploidization progressed (Fig. I-7e, f). The cell number in the cell proliferation zone was 38 for hexaploid-1, 41 for hexaploid-2, 31 for octoploid-1, and 33 for octoploid-2.

Whole-mount fluorescence *in situ* hybridization (WM-FISH) analysis of *A. thaliana* autopolyploids

I established a novel technique for the WM-FISH analysis of the whole roots of *A. thaliana* to reveal the changes in chromosome behavior due to polyploidization. The novel WM-FISH analysis clearly detected fluorescent signals at the centromeres and nuclei in the cortical cell files of *A. thaliana* (Fig. I-4) and was applicable to the autopolyploid series (Fig. I-8).

On the basis of the results of the root growth analysis, WM-FISH data were obtained for the following four growth regions: the region between the QC and the point where the LCPR decreases to 0 was defined as the cell proliferation zone (P); the region between the point where the LCPR decreases to 0 and the point at which REGR peaked, indicative of the highest relative cell growth rate, was defined as growth zone-1 (G1); the region between the point at which REGR peaked and the point where the REGR decreased to 0 was defined as growth zone-2 (G2); and the region beyond the point at which REGR decreased to 0 was defined as the mature zone (M) (Table 1).

Nuclear volume

Diploids and tetraploids had a similar nuclear volume spatial pattern, with a gradual increase from the apical region to the basal region (Fig. 9a). Overall, the nuclear volume was greater for the tetraploids than for the diploids; in the M region, the nuclei of the tetraploids were 1.73- to 1.82-times larger than those of the diploids. The spatial pattern of the nuclear volume of the high-polyploids (hexaploids and octoploids) differed from that of the diploids and tetraploids; the nuclear volume almost reached a plateau in the G2 and M regions (Fig. I-9a;

Table 1). In terms of the whole root, the hexaploids and octoploids had almost the same nuclear volume spatial profile, whereas the octoploids had a slightly larger nuclear volume than the hexaploids in the region approximately 500–1,500 μm from the QC. Interestingly, although the basic genome content was higher in the hexaploids and octoploids than in the diploid, the nuclear volumes in the mature zone were similar (i.e., only 1.04- to 1.15-times greater in the hexaploids and 0.94- to 1.15-times greater in the octoploids than in the diploid).

Degree of chromosome polytenization

The number of centromere signals may be used to estimate the degree of chromosome polytenization because the number of centromere signals reportedly decreases in nuclei with polytenized chromosomes (Breuer et al., 2007; Kikuchi and Iwamoto, 2020). Diploids and tetraploids had similar spatial patterns in the number of centromere signals, which was nearly constant in the whole root, but it was slightly higher in the cell proliferation zone (P) than in the other growth zones (the volume growth zone-1, volume growth zone-2 and mature zone) (Fig. I-9b; Fig. I-10a, b; Table 1). This result suggests that chromosome polytenization occurs in diploids and tetraploids because of the non-separation of duplicated sister chromatids in endoreduplicated nuclei. The number of centromere signals in each of the four designated regions of the diploids and tetraploids was as follows (mean ± standard error): 9.02 ± 0.09 (diploid, P), 8.09 ± 0.09 (diploid, G1), 8.29 ± 0.10 (diploid, G2), and 8.67 ± 0.27 (diploid, M) (Fig. I-10a); 17.3 ± 0.2 (tetraploid, P), 14.1 ± 0.2 (tetraploid, G1), 14.3 ± 0.2 (tetraploid, G2), and 14.6 ± 0.4 (tetraploid, M) (Fig. I-10b).

In the hexaploids and octoploids, the number of centromere signals was significantly lower in the volume growth zone-1, volume growth zone-2, and

mature zone than in the cell proliferation zone (Fig. I-9b; Fig. I-10c, d; Table 1). This result indicates that chromosome polytenization occurs in hexaploids and octoploids because of the non-separation of duplicated sister chromatids and the additional adhesion of chromosomes in endoreduplicated nuclei. The number of centromere signals in each of the four designated regions of the hexaploids and octoploids was as follows (mean ± standard error): 26.4 ± 0.2 (hexaploid, P), 19.7 ± 0.5 (hexaploid, G1), 18.2 ± 0.3 (hexaploid, G2), and 19.8 ± 0.4 (hexaploid, M) (Fig. I-10c); 33.9 ± 0.3 (octoploid, P), 24.3 ± 0.8 (octoploid, G1), 21.7 ± 0.4 (octoploid, G2), and 25.1 ± 0.6 (octoploid, M) (Fig. I-10d).

Discussion

Progression of polyploidization suppresses cell proliferation

The root growth analysis showed that local cell production rate (LCPR) decreased in the cell proliferation zone as the polyploidization progressed (Fig. I-6d, e, f). Because LCPR represents the number of cells produced at a specific location (per hour), the study data indicate that polyploids, especially high-polyploids, have a longer cell cycle than diploids. These results are consistent with those of previous studies that revealed the strong positive correlation between the genome size and the duration of the cell cycle (Hof and Sparrow, 1963; Bennett et al., 1972; Francis et al., 2008). Earlier research confirmed the cell cycle duration is primarily determined by the S phase (Francis et al., 2008; Šímová and Herben, 2012). The duration of the S phase will be constrained by the total amount of DNA and the transport rate of the components required for DNA replication (e.g.,

DNA polymerase) (Šímová and Herben, 2012). Such constraints may also occur in polyploids, which have a larger genome than diploids.

The graph plotting the LCPR against the cell number from the QC showed that the number of cells in the cell proliferation zone decreased significantly as the ploidy level increased (Fig. I-7d, e, f). Considering the size of the cell proliferation zone was almost the same in the diploid and the polyploids (Fig. I-6d, e, f), the results in Fig. I-7 indicate that the cell size in the cell proliferation zone increased as the ploidy level increased. Therefore, there is a trade-off between cell proliferation and cell volume increase in the cell proliferation zone, which Iwamoto et al. (2006) proposed following their kinematic analysis of the root growth of several *A. thaliana* ecotypes.

Tetraploidization promotes cell volume increase, whereas further polyploidizations have the opposite effect

The findings of the root growth analysis showed that the increase in cell volume in the steady-state growth region due to polyploidization occurred in tetraploids, but not in the high-polyploids (Fig. I-5g–i). However, the spatial pattern of the relative elongation rate (REGR) was almost the same for the tetraploids and diploids (Fig. I-6a), suggesting that the cortical cell file of the tetraploids likely has fewer cells than the corresponding region of the diploid, but the growth rate of each cell is probably higher in the tetraploids than in the diploid. The volume growth zone and the REGR peak were significantly smaller in the high-polyploids than in the diploid and tetraploids (Fig. I-6a–c), indicating that the cell volume increase in the high-polyploids was severely suppressed in the volume growth zone of the root. The decrease in the cell volume and volume

increase as polyploidization progresses may be caused by several physical factors, but the most likely factor is the change in the cell wall composition of high-polyploids. As polyploidization progresses, the cell wall thickness decreases in the stem and the vascular bundle tissue becomes abnormal. More specifically, octoploids have a significantly thinner cell wall than diploids, tetraploids, and hexaploids and they also have a relatively high percentage of abnormal vessels in their vascular tissue (Corneillie et al., 2019). The physical changes (e.g., decreased thickness) to the cell wall of high-polyploids may be among the main factors associated with the decrease in the cell volume and volume growth rate in high-polyploids. Corneillie et al. (2019) also revealed that the cell wall composition changes in the stem of high-polyploids, which may also influence the cell volume and volume growth rate. The thickness of the cell wall and the cell wall composition in the roots of polyploids should be more comprehensively examined in future studies to confirm this hypothesis.

As discussed in the previous section, the polyploids underwent fewer cell divisions than the diploids, but their cell volumes increased in the cell proliferation zone. Additionally, the increased genome content of the tetraploids resulted in increased cell volumes in the volume growth zone, which was in contrast to the suppressed cell volume increase in the hexaploids and octoploids. These results imply the mechanism that suppresses cell volume increase counteracts the beneficial effects of the increased genomic content due to polyploidization in high-polyploids. The whole-mount fluorescence *in situ* hybridization (WM-FISH) analysis of the chromosome dynamics in the whole root elucidated the mechanism underlying the suppressed cell growth in high-polyploids, which will be discussed in detail in the following sections.

Relationships among the nuclear volume, endoreduplication, and cell volume increase

An earlier fluorescence-activated nuclear sorting analysis showed that there are 2C, 4C, 8C, and 16C cells in the root cortical cell files in the diploid *Arabidopsis thaliana* (Bhosale et al., 2018). Thus, I speculated that the mature zone of the diploids contained 16C cells and that the cortical cells of the diploids undergo three rounds of endoreduplication (i.e., 2C to 4C to 8C to 16C; Figure I-9a). Because the DNA content of nuclei is proportional to the nuclear volume (Jovtchev et al., 2006), I predicted that the mature zone of the tetraploids comprised 32C cells. In addition, the nuclear volume in the mature zone was approximately 2-times larger in the tetraploids than in the diploid (Figure I-9a). Hence, the cortical cells of the tetraploids also undergo three rounds of endoreduplication (i.e., 4C to 8C to 16C to 32C). The progression of endoreduplication is believed to be closely related to an increase in the cell volume (Sugimoto-shirasu and Robert, 2003). Therefore, the larger cell volume and higher volume growth rate in the tetraploids than in the diploids may be attributed to the increased DNA content due to endoreduplication (Fig. I-5g).

Although the nuclear volumes in the cell proliferation zone and the volume growth zone were larger in the hexaploids and octoploids than in the diploids, the nuclear volumes in the mature zone were almost the same in the hexaploids, octoploids, and diploids (Fig. I-9a). Accordingly, most of the cortical cells in the hexaploids and octoploids likely undergo only one round of endoreduplication (i.e., 6C to 12C in hexaploids and 8C to 16C in octoploids). Moreover, the progression of endoreduplication is likely suppressed in high-polyploids (relative to the corresponding progression in diploids and tetraploids).

If the increase in the cell volume of high-polyploids was proportional to the increase in the endoploidy level of cells, the cell volume of high-polyploids at 1,000 μm from the QC should be approximately double that of the diploid because the endoploidy level (nuclear volume) of the high-polyploids at 1,000 μm from the QC was approximately double that of the diploid (Fig. I-9a). However, the kinematic analysis showed that the cell volume at 1,000 μm from the QC was not 2-times higher in the high-polyploids than in the diploids (Fig. I-5h, i). Therefore, suppressed endoreduplication cannot fully explain the suppression of cell volume increase in the high-polyploids. The contribution of chromosome polytenization is discussed in the following section.

Chromosome polytenization suppresses cell volume increase, but not cell proliferation, in high-polyploids

According to the WM-FISH analysis, chromosome polytenization was relatively rare in the cell proliferation zone of the diploid and all autopolyploids. More specifically, the number of centromere signals in the cell proliferation zone was almost the same as the number of chromosomes in the diploid and each polyploid (Fig. I-9b, I-10). Thus, it is unlikely that chromosome polytenization significantly affected the suppression of cell proliferation in the polyploids (Fig. I-6d–f); however, it is possible that a few cells with polytenized chromosomes can influence cell proliferation. Kikuchi and Iwamoto (2020) revealed extensive chromosome polytenization in polyploid leaf cells with a basic genome (i.e., 4C in tetraploids, 6C in hexaploids, and 8C in octoploids), suggesting that the cell proliferation of polyploids may be suppressed by this polytenization in leaves. The results demonstrated that this suppression does not occur, at least not in the

cortical cell files. Notably, even though the cells in the cell proliferation zone should not undergo endoreduplication, in a few nuclei, the number of centromere signals was greater than the expected number of chromosomes (diploid, 10; tetraploid, 20; hexaploid, 30; octoploid, 40). This may have been caused by the inappropriate segmentation of centromere fluorescence. In the WM-FISH analysis performed in this study, I set a threshold for each confocal image to segment the centromere fluorescence for the construction of 3D images. Although the threshold appropriately segmented most of the centromere-localized fluorescent signals, there were a few indistinct fluorescent signals that may have been inappropriately segmented into two signals. Even though I could detect these incorrectly segmented fluorescent signals, arbitrarily re-segmenting them is likely inappropriate. Because there were relatively few nuclei in which the number of centromere signals exceeded the expected number of chromosomes (Fig. I-10), I concluded that the influence of inappropriate segmentation was negligible. Nevertheless, I will need to improve the quality of the confocal images and the method used for segmenting fluorescent signals in future studies.

The degree of chromosome polytenization in the volume growth zone and mature zone differed among the diploids and polyploids (Fig. I-9b; Fig. I-10). Although there was a significant difference between the cell proliferation zone and volume growth zone-1 in the diploid and all polyploids (Fig. I-10), the degree of the decrease in the centromere signals was proportional to the ploidy level. The number of centromere signals in the volume growth zone-1 of the high-polyploids decreased significantly by approximately 40% (compared with the number of centromere signals in the cell proliferation zone). In the high-polyploids, the number of centromere signals decreased further in the volume growth zone-2. In contrast, there was no significant difference in the number of

centromere signals between the volume growth zone-1 and volume growth zone-2 in the diploid and tetraploids (Fig. I-10). These results reflected the extensive chromosome polytenization in the high-polyploids, which helps explain the decreased cell volume and volume growth rate observed in the high-polyploids (Fig. I-5g, h, i). Changes in the chromatin structure lead to altered gene expression (Ojolo et al., 2018). The chromosome polytenization may be related to modified chromatin structures, resulting in gene expression changes in the volume growth zone and mature zone of the high-polyploids. Indeed, the diversity in chromosome structures reportedly explains the differences in gene expression between autotetraploid *A. thaliana* and its diploid counterpart (Zhang et al., 2019).

Future studies should focus on the chromosome dynamics associated with the progression of polyploidization. In particular, a single-nucleus ATAC-sequencing analysis may provide insights into the effects of chromatin accessibility on gene expression (Farmer et al. 2021), while also elucidating the relationship between chromosome polytenization and repressed gene expression in high-polyploids. A Hi-C sequencing analysis should also be conducted to generate a map of the three-dimensional genome organization in the *A. thaliana* root (Wang et al. 2015) and reveal how chromosome polytenization in high-polyploids modulates the genome organization and affects gene expression. Before completing the ATAC-sequencing and Hi-C sequencing analyses, I plan on analyzing the transcriptome of each root region in diploids and polyploids to verify that chromosome polytenization influences gene expression. If changes in gene expression among diploids, tetraploids, and high-polyploids are detected, it may be possible to identify the genes responsible for the growth changes due to

chromosome polytenization by comparing the transcriptome sequencing data with the results of the kinematic analysis of *A. thaliana* root growth.

Concluding remarks

In this study, I analyzed the spatial pattern of each growth parameter by performing a kinematic analysis of cells. A comparison with diploids indicated that tetraploidization promotes cell volume increase and suppresses cell proliferation. The kinematic analysis also showed that the suppression of cell proliferation and cell volume increase significantly inhibits the growth of high-polyploids. I also established a novel method for performing WM-FISH analyses and examined the spatial patterns of the degree of chromosome polytenization. The endoploidy level estimated on the basis of the nuclear volume indicated that high-polyploids undergo fewer endoreduplication cycles than diploids and tetraploids. The nuclear volume plateaus closer to the QC in high-polyploids than in diploids and tetraploids, which may be related to the smaller volume growth zone of high-polyploids. I also determined the number of centromere signals via a WM-FISH analysis and confirmed that chromosome polytenization did not occur in most of the cells in the volume growth zone of the diploids and polyploids. However, chromosome polytenization in the volume growth zone was more extensive in the high-polyploids than in the diploids and tetraploids. These findings suggest that chromosome polytenization is unrelated to the suppression of cell proliferation, but it does contribute to the suppression of the cell volume increase in high-polyploids (Fig. I-11).

Table I-1. Growth zone regions in *Arabidopsis thaliana* autopolyploid roots

Table 1. Range of each growth zone in autopolyploid series of *A. thaliana*

	Cell proliferation zone (P)	Growth zone-1 (G1)	Growth zone-2 (G2)	Mature zone (M)
Diploid	QC < P ≦ 350 μm	350 < G1 ≦ 825 μm	825 < G2 ≦ 2650 μm	2650 μm < M
Tetraploid	QC < P ≦ 325 μm	325 < G1 ≦ 725 μm	725 < G2 ≦ 2600 μm	2600 μm < M
Hexaploid	QC < P ≦ 275 μm	275 < G1 ≦ 700 μm	700 < G2 ≦ 1850 μm	1850 μm < M
Octoploid	QC < P ≦ 275 μm	275 < G1 ≦ 575 μm	575 < G2 ≦ 2000 μm	2000 μm < M

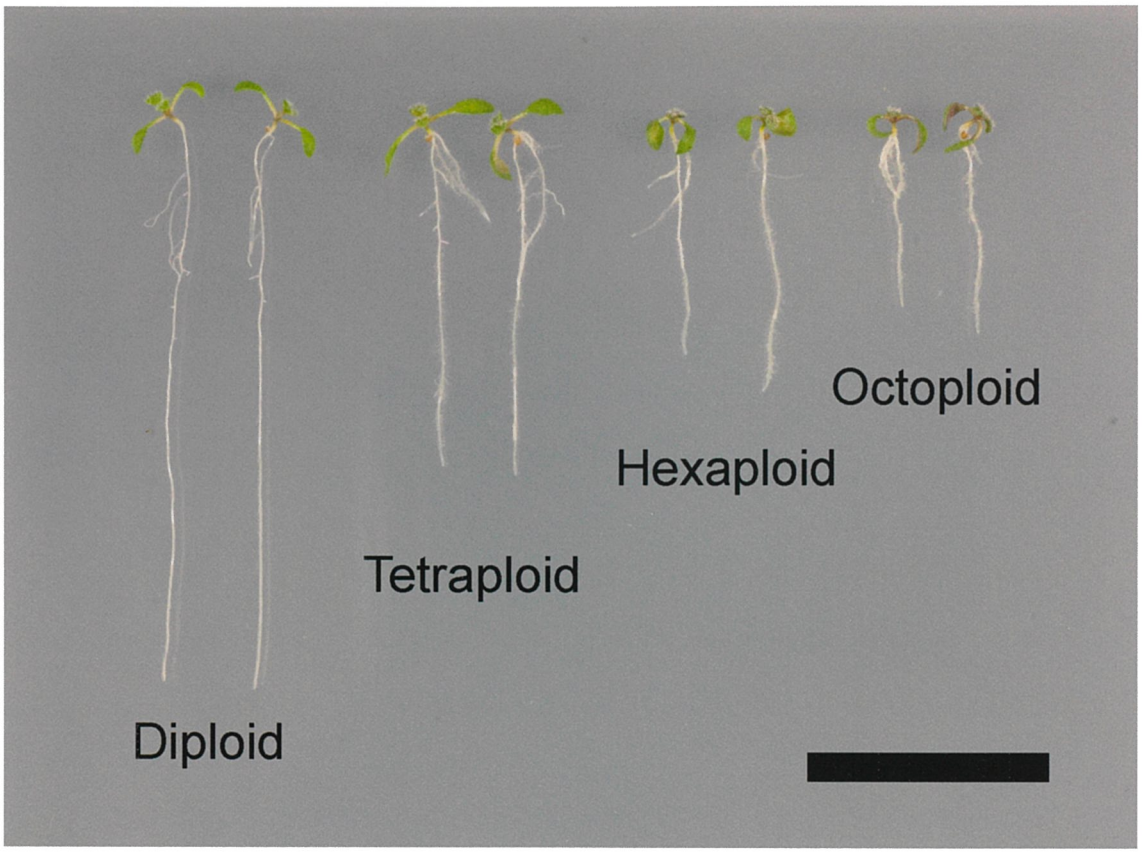

Figure I-1. *Arabidopsis thaliana* autopolyploids (diploid, tetraploid, hexaploid, and octoploid)

Eight-day-old seedlings were grown vertically on solid media containing MS salts. The length of the primary root was inversely proportional to the ploidy level. The kinematic analysis of cells was performed using the eight-day-old seedlings, which exhibited steady primary root growth. Scale bar = 2 cm

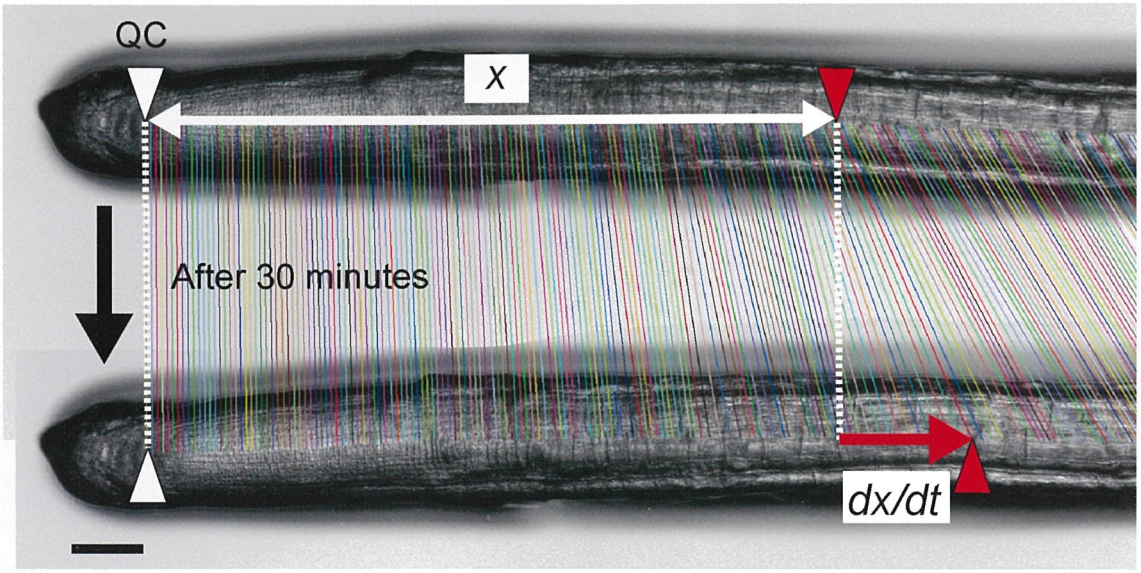

Figure I-2. Root elongation rate determined using the Neo Measure image analysis program

Two time-lapse images of the analyzed root (30 min interval) were used as the input for Neo Measure (ImageJ plugin; Iwamoto et al., in preparation). The spatial profile of the elongation rate (dx/dt) was determined by matching points in the two images. x represents the distance from the quiescent center (QC). Scale bar = 100 μm

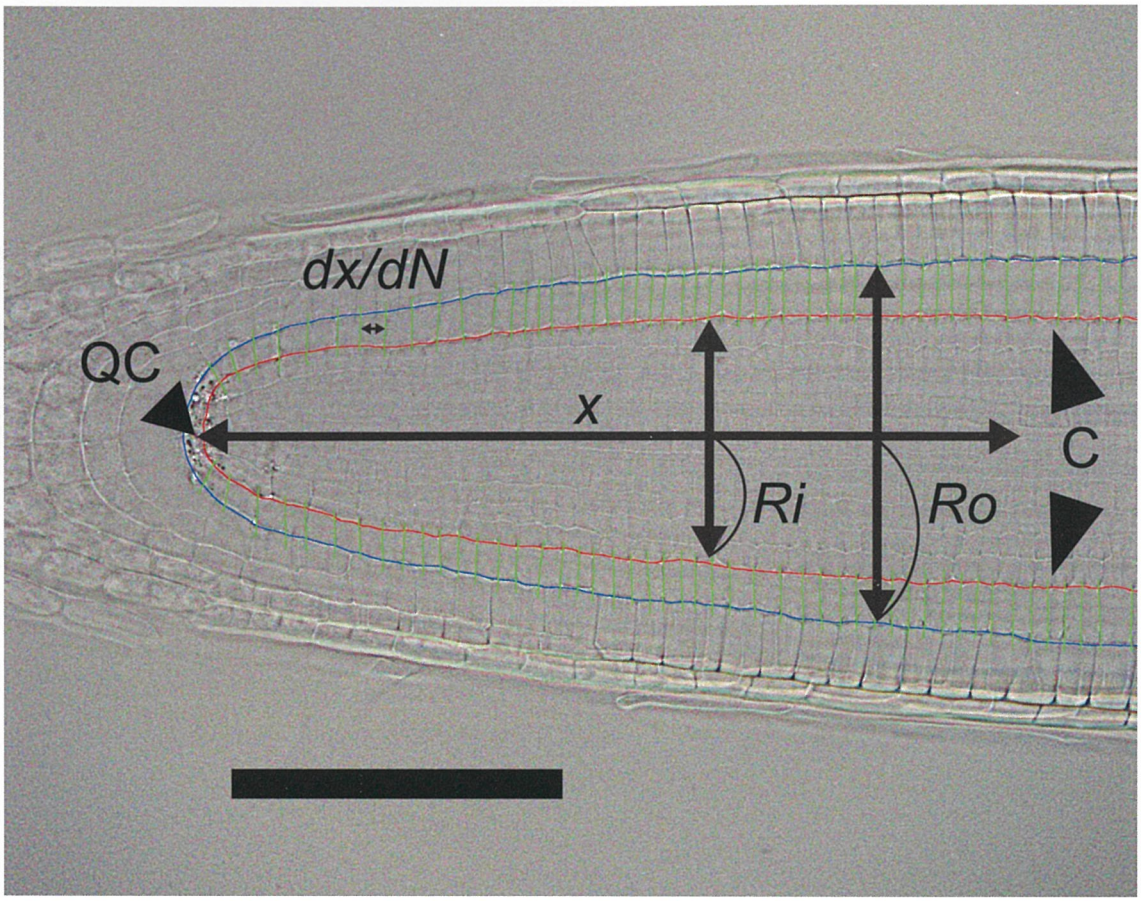

Figure I-3. Measurement of the cell length using the Root Cell Size Measurer image analysis program

Cleared root for measuring the cell length (*dx/dN*) in the cortical cell file (C). *x* represents the distance from the QC. The inner radius (*Ri*) and outer radius (*Ro*) of the cortical cell file were also measured for the same root for the length-to-volume conversion. Scale bar = 100 μm

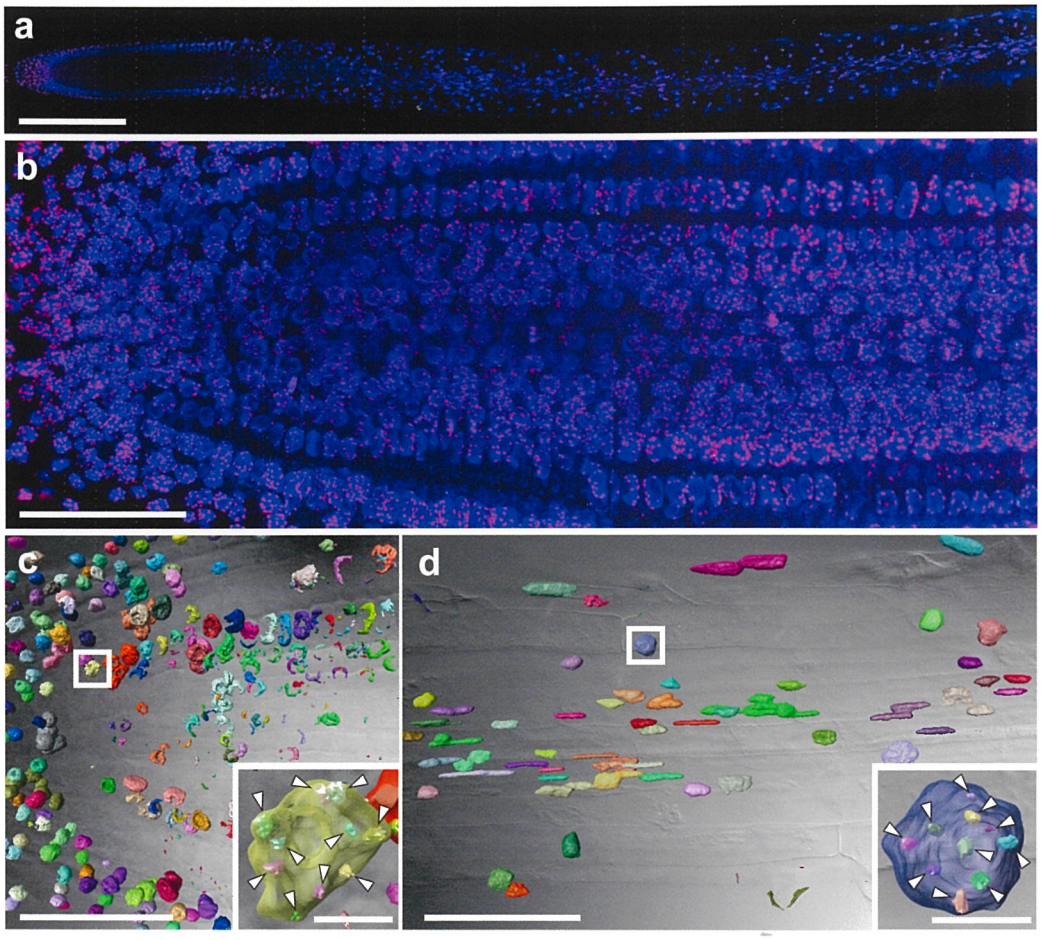

Figure I-4. Whole-mount FISH (WM-FISH) analysis of the *A. thaliana* root tip

(a) WM-FISH image of the intact root tip (magnification ×40). Red signals, centromeres labeled with Cy3; blue signals, nucleus stained with DAPI. (b) Magnified view of the apical region close to the QC of the analyzed root in (a) (magnification ×100). (c) 3D image of the nuclei in the apical region of the root. (d) 3D image of the nuclei in the basal region of the root. Confocal images from the WM-FISH analysis (a, b) were converted to 3D images using Amira software (Mercury Computer Systems, Berlin, Germany) (c, d). Cortical cell files in the 3D image were identified using differential interference contrast images. Inserts in (c) and (d) present an enlarged image of the nucleus surrounded by a white square. These images are superimposed images of nuclei and centromere signals. Arrowheads indicate the centromere signals. Scale bars = 300 μm (a), 100 μm (b, d), 50 μm (c), 3 μm (insert in c), and 10 μm (insert in d)

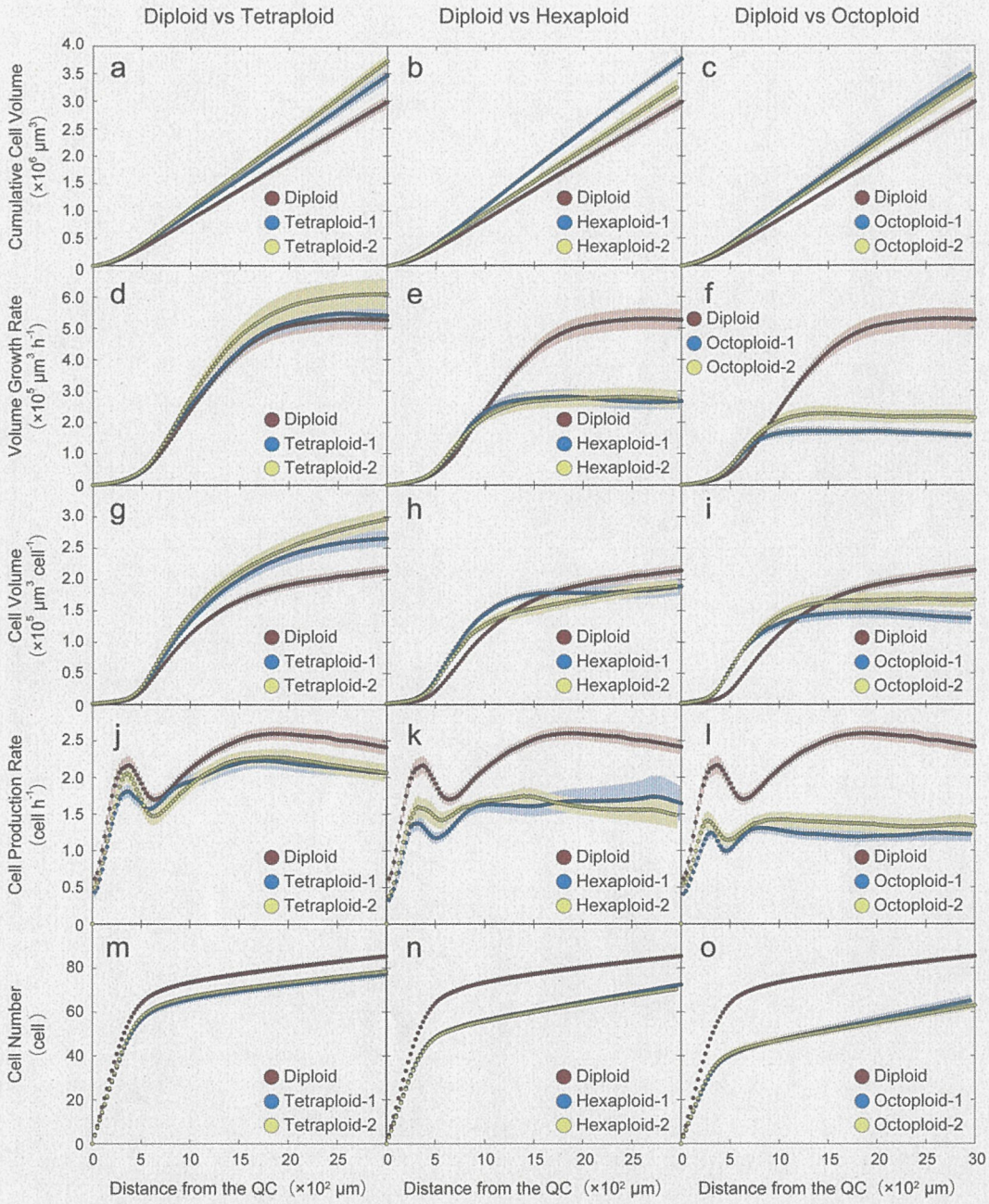

Figure I-5. Spatial profiles of the root growth parameters of *A. thaliana* autopolyploids

Data were plotted versus the distance from the QC. (a–c) Cumulative cell volume. (d–f) Volume growth rate. (g–i) Cell volume. (j–l) Cell production rate. (m–o) Cell number. Data for the diploids were identical for (a–c), (d–f), (g–i), (j–l), and (m–o). Bars indicate standard errors. n = 40 (diploid); n = 30 (other strains)

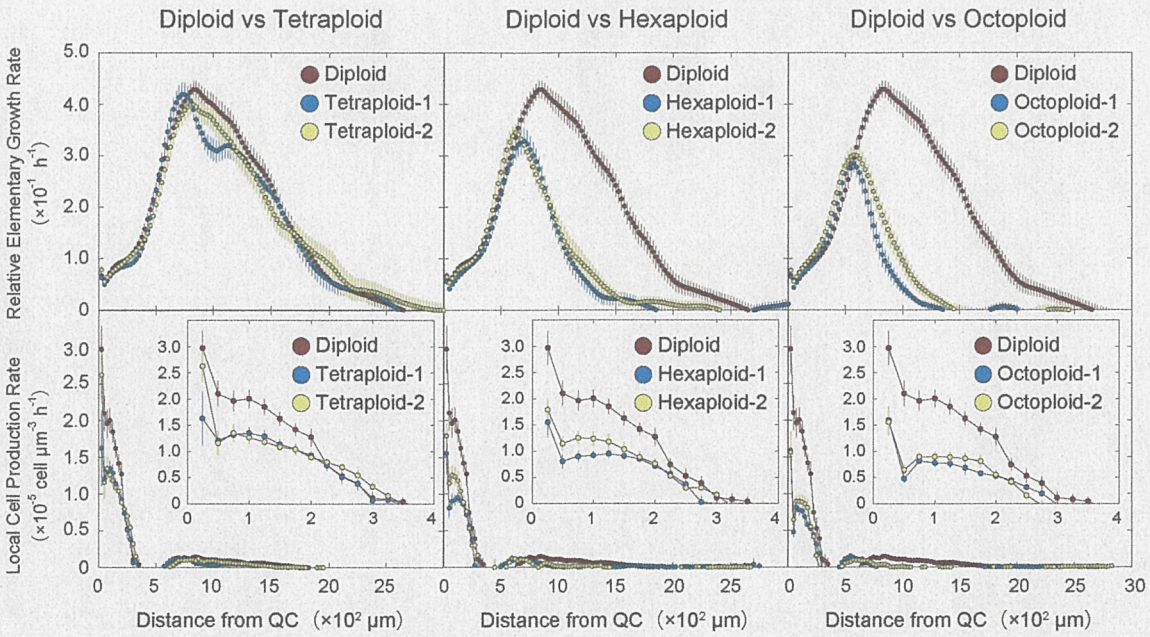

Figure I-6. Spatial profiles of REGR and LCPR for the *A. thaliana* autopolyploids

Data were plotted versus the distance from the QC. (a–c) Relative elongation growth rate (REGR). (d–f) Local cell production rate (LCPR). Insets present the spatial profiles of LCPR in the region close to the QC. Data for the diploids were identical for (a–c) and (d–f). Bars indicate standard errors. n = 40 (diploid); n = 30 (other strains)

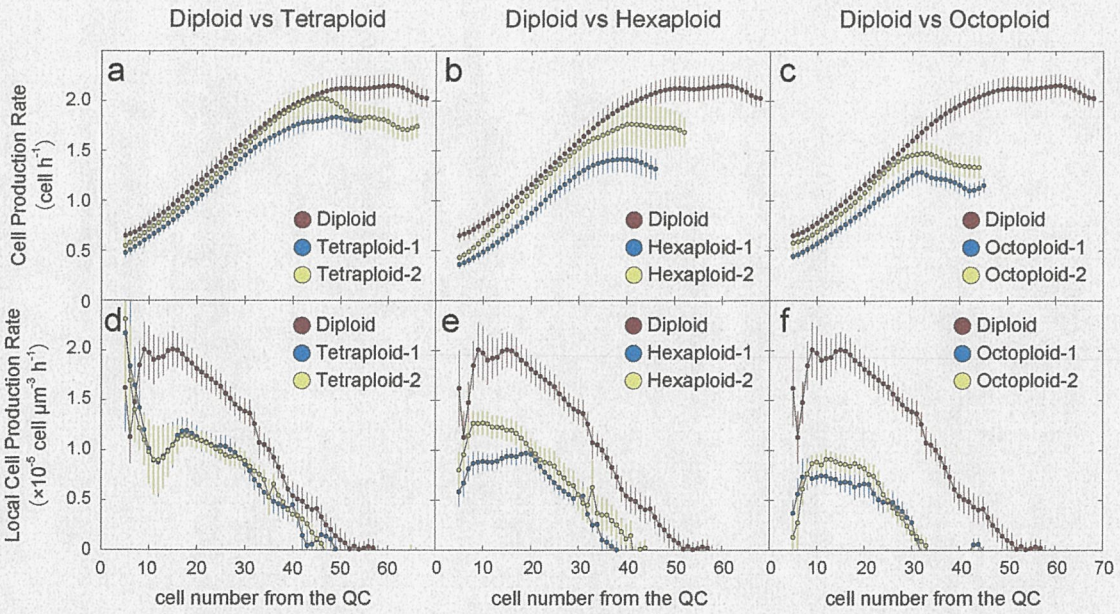

Figure I-7. Spatial profiles of the cell production rate and LCPR for the *A. thaliana* autopolyploids

Data were plotted versus the cell number from the QC. (a–c) Cell production rate. (d–f) Local cell production rate (LCPR). Data for the diploids were identical for (a–c) and (d–f). Bars indicate standard errors. n = 40 (diploid); n = 30 (other strains)

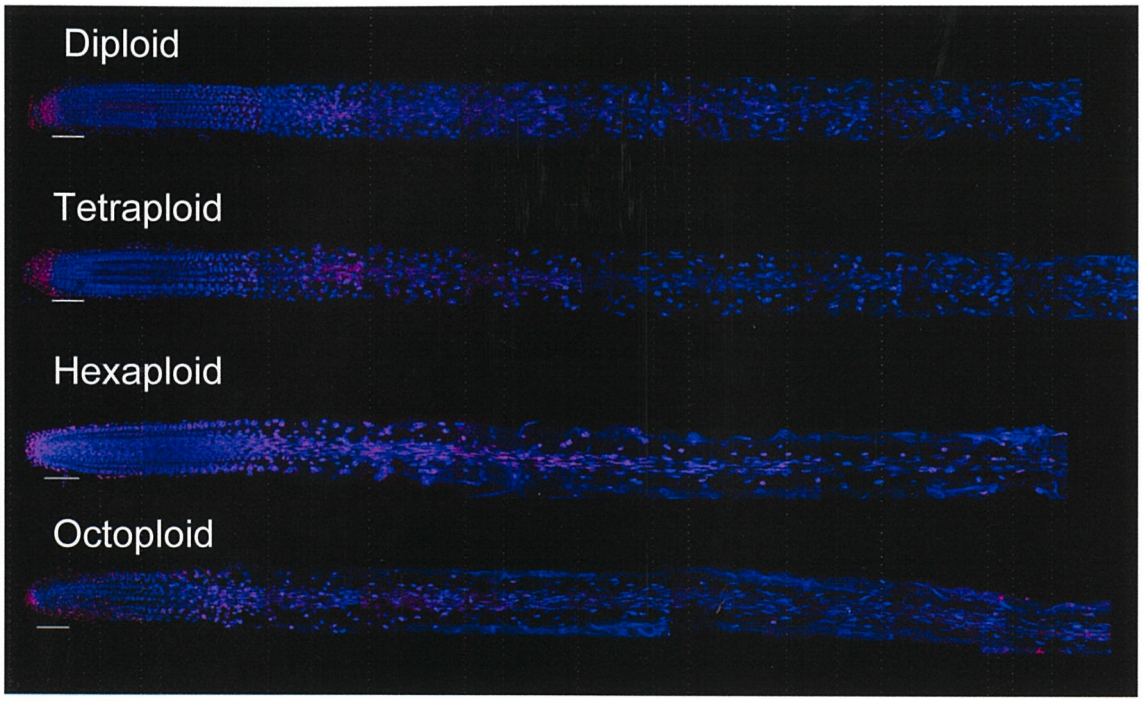

Figure I-8. Confocal images of the whole-mount FISH (WM-FISH) analysis

The novel WM-FISH technique successfully detected fluorescent DAPI (nuclei) and Cy3 (centromere) signals in each region of the intact root of *A. thaliana* autopolyploids. Scale bars = 100 μm

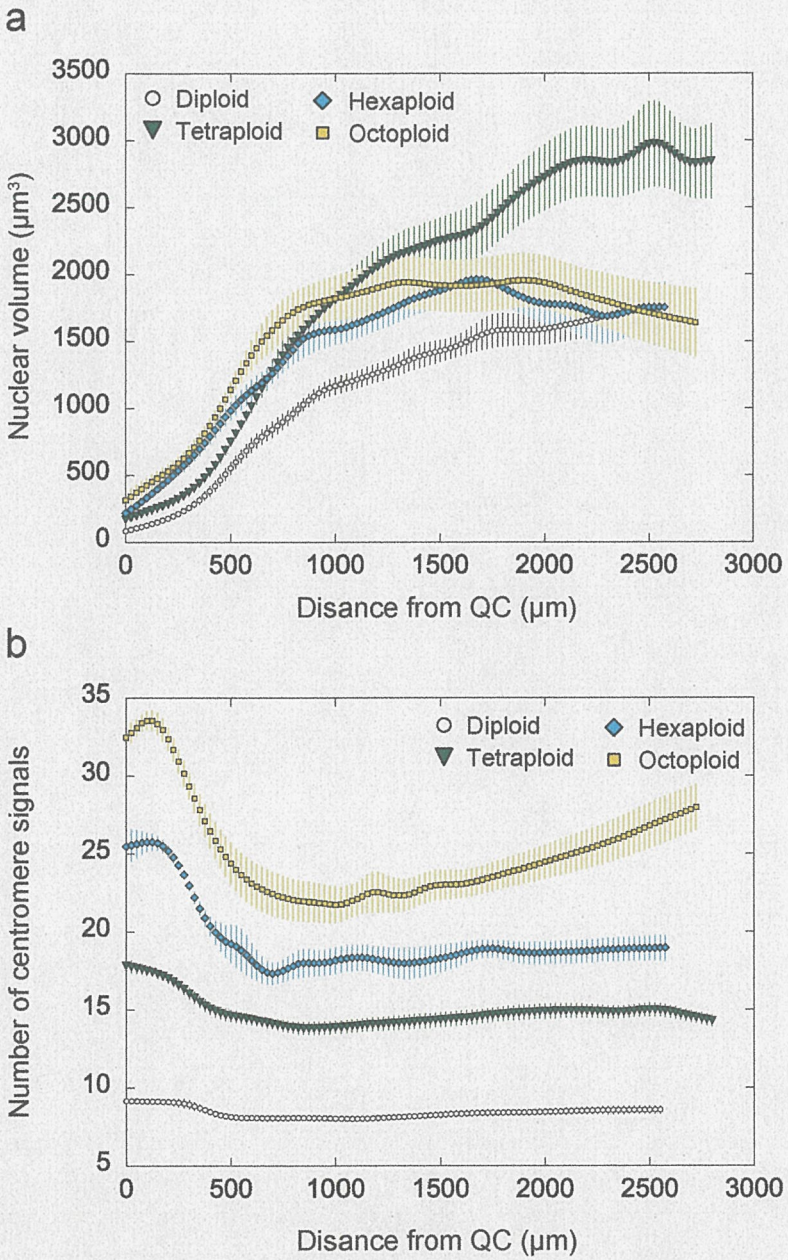

Figure I-9. Whole-mount FISH (WM-FISH) analysis of the root tip of *A. thaliana* autopolyploids

Data were plotted versus the distance from the QC. (a) Nuclear volume. (b) Number of centromere signals. Bars indicate standard errors. n = 10 (each strain). For (a) and (b), graphs present the fitted curves obtained by smoothing (Friedman super smoother) and interpolating (spline interpolation) the raw data of the number of centromere signals and nuclear volume, respectively

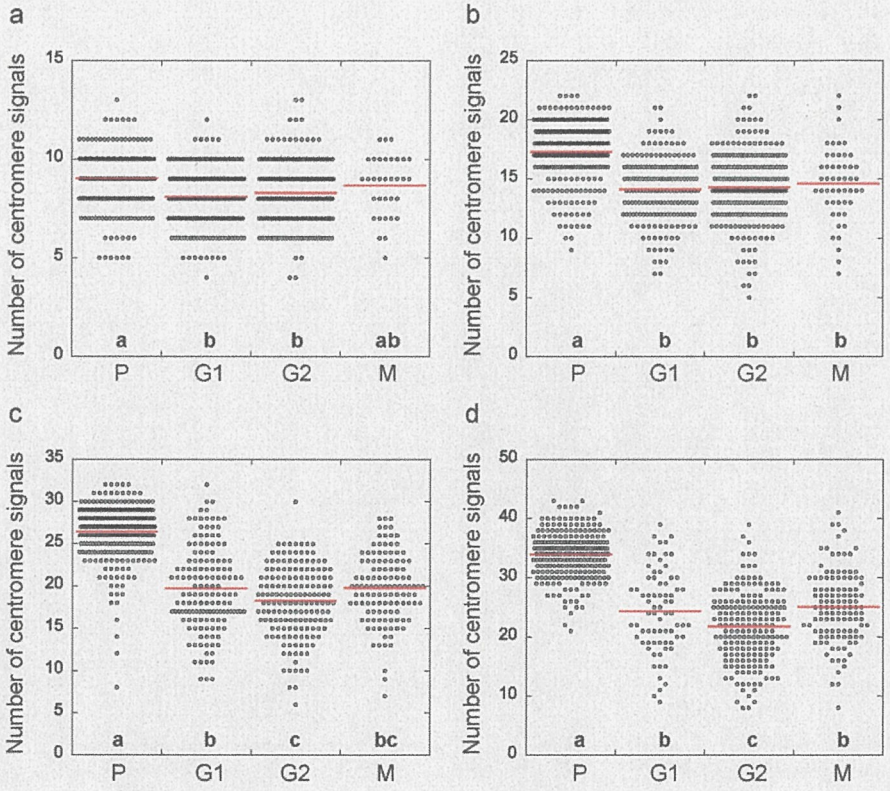

Figure I-10. One-dimensional scatter plot of the number of centromere signals in the nucleus of each strain

(a) Diploid: n = 245 (P, cell proliferation zone), 248 (G1, volume growth zone-1), 238 (G2, volume growth zone-2), and 33 (M, mature zone). (b) Tetraploid: n = 261 (P), 178 (G1), 234 (G2), and 50 (M). (c) Hexaploid: n = 304 (P), 144 (G1), 164 (G2), and 119 (M). (d) Octoploid: n = 237 (P), 73 (G1), 194 (G2), and 118 (M). Red lines represent the mean. The number of centromere signals in each region of each strain was as follows (mean ± standard error): 9.02 ± 0.09 (diploid, P), 8.09 ± 0.09 (diploid, G1), 8.29 ± 0.10 (diploid, G2), and 8.67 ± 0.27 (diploid, M) (Fig. I-10a); 17.3 ± 0.2 (tetraploid, P), 14.1 ± 0.2 (tetraploid, G1), 14.3 ± 0.2 (tetraploid, G2), and 14.6 ± 0.4 (tetraploid, M) (Fig. I-10b); 26.4 ± 0.2 (hexaploid, P), 19.7 ± 0.5 (hexaploid, G1), 18.2 ± 0.3 (hexaploid, G2), and 19.8 ± 0.4 (hexaploid, M) (Fig. I-10c); 33.9 ± 0.3 (octoploid, P), 24.3 ± 0.8 (octoploid, G1), 21.7 ± 0.4 (octoploid, G2), and 25.1 ± 0.6 (octoploid, M) (Fig. I-10d). Different letters indicate significant differences in the mean values ($p < 0.05$) (a, b: Tukey HSD post hoc test; c, d: Steel-Dwass test)

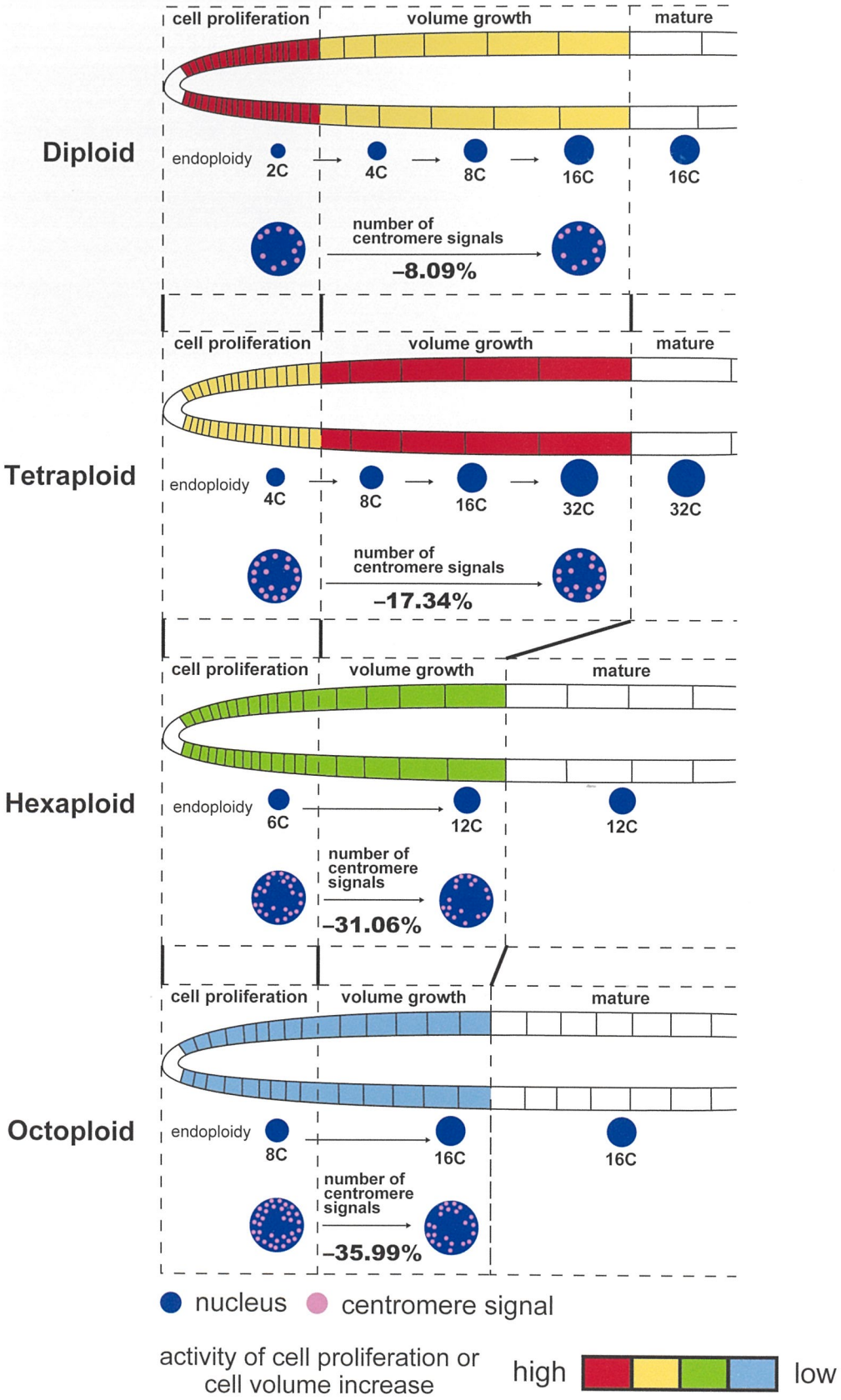

Figure I-11. Summary of Chapter 1

References

Beemster GTS, Baskin TI (1998) Analysis of cell division and elongation underlying the developmental acceleration of root growth in *Arabidopsis thaliana*. *Plant Physiology* **116**:1515–1526. https://doi.org/10.1104/pp.116.4.1515

Bennett MD, Smith JB, Riley R (1972) The effects of polyploidy on meiotic duration and pollen development in cereal anthers. *Proceedings of the Royal Society of London Series B Biological Sciences* **181**:81–107. https://doi.org/10.1098/rspb.1972.0041

Berr A, Schubert I (2007) Interphase chromosome arrangement in *Arabidopsis thaliana* is similar in differentiated and meristematic tissues and shows a transient mirror symmetry after nuclear division. *Genetics* **176**:853–863. https://doi.org/10.1534/genetics.107.073270

Bhosale R, Boudolf V, Cuevas F, Lu R, Eekhout T, Hu Z, Van Isterdael G, Lambert GM, Xu F, Nowack MK, Smith RS, Vercauteren I, De Rycke R, Storme V, Beeckman T, Larkin JC, Kremer A, Höfte H, Galbraith DW, Kumpf RP, Maere S, De Veylder L (2018) A Spatiotemporal DNA endoploidy map of the Arabidopsis root reveals roles for the endocycle in root development and stress adaptation. *The Plant Cell* **30**:2330–2351. https://doi.org/10.1105/tpc.17.00983

Breuer C, Stacey NJ, West CE, Zhao Y, Chory J, Tsukaya H, Azumi Y, Maxwell A, Roberts K, Sugimoto-Shirasu K (2007) BIN4, a novel component of the plant DNA topoisomerase VI complex, is required for endoreduplication in *Arabidopsis*. *The Plant Cell* **19**:3655–3668. https://doi.org/10.1105/tpc.107.054833

Corneillie S, De Storme N, Van Acker R, Fangel JU, De Bruyne M, De Rycke R, Willats WGT, Vanholme B, Boerjan W (2019) Polyploidy Affects Plant Growth and Alters Cell Wall Composition. *Plant Physiology* **179**:74–87. https://doi.org/10.1104/pp.18.00967

Dolan L, Janmaat K, Willemsen V, Linstead P, Poethig S, Roberts K, Scheres B (1993) Cellular organisation of the *Arabidopsis thaliana* root. *Development* **119**:71–84. https://doi.org/10.1242/dev.119.1.71

Erickson RO (1976) Modeling of Plant-Growth. *Annual Review of Plant Physiology and Plant Molecular Biology* **27**:407–434. https://doi.org/10.1146/annurev.pp.27.060176.002203

Farmer A, Thibivilliers S, Ryu KH, Schiefelbein J, Libault M (2021) Single-nucleus RNA and ATAC sequencing reveals the impact of chromatin accessibility on gene expression in Arabidopsis roots at the single-cell level. *Molecular Plant* **14**:372–383. https://doi.org/10.1016/j.molp.2021.01.001

Francis D, Davies MS, Barlow PW (2008) A strong nucleotypic effect on the cell cycle regardless of ploidy level. *Annals of Botany* **101**:747–757. https://doi.org/10.1093/aob/mcn038

Friedman JH (1984) A variable span scatterplot smoother. *Laboratory for Computational Statics, Stanford University Technical Report* **5**.

Hof JV, Sparrow AH (1963) A relationship between DNA content, nuclear volume, and minimum mitotic cycle time. *Proceedings of the National Academy of Sciences* **49**:897–902. https://doi.org/10.1073/pnas.49.6.897

Iwamoto A, Satoh D, Furutani M, Maruyama S, Ohba H, Sugiyama M (2006) Insight into the basis of root growth in *Arabidopsis thaliana* provided by a simple mathematical model. *Journal of plant research* **119**:85–93. https://doi.org/10.1007/s10265-005-0247-x

Jarillo JA, Piñeiro M, Cubas P, Martínez-Zapater JM, Jarillo JA, Piñeiro M, Cubas P, Martínez-Zapater JM (2009) Chromatin remodeling in plant development. *International Journal of Developmental Biology* **53**:1581–1596. https://doi.org/10.1387/ijdb.072460jj

Johnston JS, Bennett MD, Rayburn AL, Galbraith DW, Price HJ (1999) Reference standards for determination of DNA content of plant nuclei. *American Journal of Botany* **86**:609–613. https://doi.org/10.2307/2656569

Jovtchev G, Schubert V, Meister A, Barow M, Schubert I (2006) Nuclear DNA content and nuclear and cell volume are positively correlated in angiosperms. *Cytogenetic and Genome Research* **114**:77–82. https://doi.org/10.1159/000091932

Kikuchi S, Iwamoto A (2020) Quantitative analysis of chromosome polytenization in synthetic autopolyploids of *Arabidopsis thaliana*. *Cytologia* **85**:189–195. https://doi.org/10.1508/cytologia.85.189

Kikuchi S, Iwamoto A (2021) An efficient method of tetraploid and octaploid induction in *Arabidopsis thaliana* using colchicine treatment. *Science Journal of Kanagawa University* **32**:81–86.

Kozlova L, Petrova A, Ananchenko B, Gorshkova T (2019) Assessment of primary cell wall nanomechanical properties in internal cells of non-fixed maize roots. *Plants* **8**:172. https://doi.org/10.3390/plants8060172

Kutsuna N, Higaki T, Matsunaga S, Otsuki T, Yamaguchi M, Fujii H, Hasezawa S (2012) Active learning framework with iterative clustering for bioimage classification. *Nature Communications* **3**:1032. https://doi.org/10.1038/ncomms2030

Ojolo SP, Cao S, Priyadarshani SVGN, Li W, Yan M, Aslam M, Zhao H, Qin Y (2018) Regulation of plant growth and development: A review from a

chromatin remodeling perspective. *Frontiers in Plant Science* **9**:1232. https://doi.org/10.3389/fpls.2018.01232

R Development Core Team (2020) R: a language and environment for statistical computing. http://www.R-project.org

Samalova M, Elsayad K, Melnikava A, Peaucelle A, Gahurova E, Gumulec J, Spyroglou I, Zemlyanskaya EV, Ubogoeva EV, Hejatko J (2020) Expansin-controlled cell wall stiffness regulates root growth in *Arabidopsis*. bioRxiv 2020.06.25.170969. https://doi.org/10.1101/2020.06.25.170969

Šímová I, Herben T (2012) Geometrical constraints in the scaling relationships between genome size, cell size and cell cycle length in herbaceous plants. *Proceedings of the Royal Society B: Biological Sciences* **279**:867–875. https://doi.org/10.1098/rspb.2011.1284

Somssich M, Khan GA, Persson S (2016) Cell wall heterogeneity in root development of *Arabidopsis*. *Frontiers in Plant Science* **7**:1242. https://doi.org/10.3389/fpls.2016.01242

Song MJ, Potter BI, Doyle JJ, Coate JE (2020) Gene balance predicts transcriptional responses immediately following ploidy change in *Arabidopsis thaliana*. *The Plant Cell* **32**:1434–1448. https://doi.org/10.1105/tpc.19.00832

Song Z-T, Liu J-X, Han J-J (2021) Chromatin remodeling factors regulate environmental stress responses in plants. *Journal of Integrative Plant Biology* **63**:438–450. https://doi.org/10.1111/jipb.13064

Sugimoto-Shirasu K, Roberts K (2003) "Big it up": endoreduplication and cell-size control in plants. *Current Opinion in Plant Biology* **6**:544–553. https://doi.org/10.1016/j.pbi.2003.09.009

Tsukaya H (2008) Controlling size in multicellular organs: focus on the leaf. *PLoS Biology* **6**:e174. https://doi.org/10.1371/journal.pbio.0060174

Verbelen J-P, Cnodder TD, Le J, Vissenberg K, Baluška F (2006) The root apex of *Arabidopsis thaliana* consists of four distinct zones of growth activities. *Plant Signaling & Behavior* **1**:296–304. https://doi.org/10.4161/psb.1.6.3511

Wang C, Liu C, Roqueiro D, Grimm D, Schwab R, Becker C, Lanz C, Weigel D (2015) Genome-wide analysis of local chromatin packing in *Arabidopsis thaliana*. *Genome Research* **25**:246–256. https://doi.org/10.1101/gr.170332.113

West G, Inze D, Beemster GTS (2004) Cell cycle modulation in the response of the primary root of *Arabidopsis* to salt stress. *Plant Physiology* **135**:1050–1058. https://doi.org/10.1104/pp.104.040022

Wolf S, Hématy K, Höfte H (2011) Growth control and cell wall signaling in plants. *Annual review of plant biology* **63**:381–407. https://doi.org/10.1146/annurev-arplant-042811-105449

Zhang H, Zheng R, Wang Y, Zhang Y, Hong P, Fang Y, Li G, Fang Y (2019) The effects of *Arabidopsis* genome duplication on the chromatin organization and transcriptional regulation. *Nucleic Acids Research* **47**:7857–7869. https://doi.org/10.1093/nar/gkz511

Chapter II. Different effects of gellan gum and agar on change in root elongation in *Arabidopsis thaliana* by polyploidization: the key role of aluminum

Abstract

I have found that agar and gellan gum have different effects on polyploidy-dependent growth alteration in *Arabidopsis thaliana*. I aimed to characterize this differential effects of agar and gellan gum and examine the physico-chemical pproperties in each gelling agent to elucidate key factors that caused the differences. Plants of each polyploid strain were cultured vertically on agar and gellan gum solidified medium. Root elongation rate was measured from 4 to10 days after sowing. The result showed that agar is favorable for root elongation of polyploids than gellan gum. Then water potential, gel hardness, and trace elements of each medium were quantified. Water potential and gel hardness of agar medium were significantly higher than those of gellan gum medium. The decrease in water potential and gel hardness in agar medium, however, did not affect the polyploidy-dependent growth alterlation. Elemental analysis showed that gellan gum contained more aluminum than agar. Subsequently, the polyploids were grown on agar media with additional aluminum, on which the root elongation in tetraploids and octoploids was significantly suppressed. These results revealed that agar and gellan gum affect the change in growth of root elongation in *A. thaliana* by polyploidization in different ways and the different effects are partially caused by aluminum in the gellan gum.

Introduction

Gelling agents are among the key ingredients that determine the characteristics of plant growth media (Debergh 1983; Kumar and Reddy 2011; Gruber et al. 2013). Agar and gellan gum are the most popular gelling agents used in plant growth media, and several studies have shown that their effects on plant growth are different.

Agar is a complex polysaccharide derived from red algae (Usov 2011) and has traditionally been used in plant growth media. Gellan gum is a bacterial polysaccharide produced using *Sphingomonas spp.* (Jansson et al. 1983), which forms transparent gels in the presence of multivalent cations (Morris et al. 2012; Kirchmajer et al. 2014). Agar media are more suitable than gellan gum media for plant growth; agar improved the growth characteristics of *Swartzia madagascariensis* (Berger and Schaffner 1995), lettuce (Ichimura and Oda 1998), and *Stevia* (Fatima and Khan 2011), and promoted the induction of shoots in certain apple varieties (Mitić 2012). However, there have also been reports of gellan gum being a more suitable ingredient for plant growth than agar, as in the case of seedling growth in cucumber (*Cucumis sativus*) (Ichi et al. 1986), shoot regeneration in *Eucomis autumnalis* (Masondo et al. 2015), shoot growth in several Australian tree species (Williams and Taji 1987), and micropropagation in *Scrophularia yoshimurae* (Tsay et al. 2006). The above reports show that the choice of a gelling agent depends upon the effect it has on growth of plant species and/or the tissue used for analysis. Both gelling agents have been widely used for growth analysis of the model plant *Arabidopsis thaliana.*

Chromosome polyploidization is very common in plants (angiosperms) and plays a significant role in their speciation (Leitch and Bennett 1997; Soltis

et al. 2003). Polyploidization affects various aspects of plant growth. In general, the cell volume of plants increases with polyploidy, resulting in an increase in organ size (Levin, 1983; Robinson et al., 2018; Corneillie et al., 2019). However, Tsukaya (2008) reported that the hexaploids and octoploids of *A. thaliana* showed suppressed growth when compared to the diploid strain. Growth suppression due to high-ploidy (i.e., hexaploidy and octoploidy) is termed "high-ploidy sydrome" (Tsukaya, 2008). Previous studies examined the effects of polyploidization on plant growth using a synthetic autopolyploid series of *A. thaliana* (Iwamoto et al., 2006 and 2013; Kikuchi and Iwamoto, 2020). They performed a kinematic analysis of the cellular basis of root growth in diploid and autotetraploid *A. thaliana* and showed that polyploidization accelerated root growth in tetraploids due to increase in volume growth rate (Iwamoto et al., 2006 and 2013). I also performed fluorescence *in situ* hybridization (FISH) analysis with a centromeric DNA probe on the leaf cells of diploid and synthetic autopolyploid series of *A. thaliana* to observe and quantify chromosome polytenization in polyploid plants (Kikuchi and Iwamoto, 2020). I observed that the degree of chromosome polytenization increased with an increase in the degree of ploidy, suggesting that the suppression of cell proliferation in the root of polyploid plants may be related to chromosome polytenization.

My preliminary observations in these previous studies showed that while the root length in 10-day-old tetraploid seedlings was longer than that of diploids on agar medium, the root length of tetraploids is shorter than that of diploids on gellan gum medium, and they also showed that hexaploids and octoploids were more severely suppressed in root growth on gellan gum medium than on agar medium (Fig. II-1). These results clearly indicate that the gelling agent influences the change in growth caused by polyploidization.

The effects of agar and gellan gum on the root growth of polyploids has been attributed to two possible factors: differences with respect to physical properties, and differences in trace elements. The physical attributes of gelling agents that affect plant growth are gel hardness (Jacques et al., 2020), water potential, and water availability of media (Buah et al. 1999; Klimaszewska et al. 2000). Further, trace elements present in gelling agents also affect plant growth (Ichimura and Oda 1998; Ichi et al. 2014; Al-Mayahi and Ali 2021).

The objective of the present study was to determine the mechanisms by which the difference in the gelling agent affected change in growth caused by polyploidization. I analyzed the effects of the two gelling agents, agar and gellan gum, on root elongation in the polyploid series of *A. thaliana.* Identifying the differences between the two gelling agents in terms of their physical properties as well as trace element content further helped us understand the effects of gelling agents on plant growth under various physical conditions. In particular, I aimed to study the effects of Al as an important trace element in agar media to elucidate its effect on root growth of polyploids.

Materials and Methods

Production of synthetic autopolyploid series of *Arabidopsis thaliana*

Synthetic autopolyploids of *A. thaliana* (tetraploid, hexaploid, and octoploid) were produced using colchicine treatment of diploid seedlings (Kikuchi and Iwamoto 2021). The ploidy level was determined by flow cytometry analysis.

Polyploid strains for which the ploidy level was confirmed for at least three generations after colchicine treatment were used in the experiment.

Flow cytometry analysis

Leaf samples for flow cytometry analysis were collected from seedlings 30–40 days after sowing (DAS) to produce polyploids and 10–15 DAS for the measurement of root elongation rate. Ploidy of each strain was confirmed with a flow cytometer (CyFlow Ploidy Analyzer PA, Münster, Germany) using the chopping method (Johnston et al. 1999).

Plant material and growth conditions

Seeds of the autopolyploid series (diploid, tetraploid, hexaploid, and octoploid) of *A. thaliana* ecotype Columbia were surface sterilized with 20 % (v/v) sodium hypochlorite and 0.5 % (v/v) Triton X-100. The seeds were sown in each growth medium and placed vertically for 10 days under constant conditions (22 °C, continuous light 90 μmol m^{-2} s^{-1}). All the growth media used in this study contained the following common components: 10 g sucrose, 0.5 g 2-Morpholinoethanesulfonic acid, 10 mL Murashige and Skoog (MS) vitamin (10.0 mg/L of thiamine, 0.5 mg/L pyridoxine, 0.5 mg/L nicotinic acid, and 100 mg/L inositol), and 2.3 g MS Plant Salt Mixture (Wako Pure Chemical Industries, Osaka, Japan) in 1 L. The gellan gum solidified media contained 0.8 % (w/v) gellan gum (Lot #SLBV6512, G1910-250G, Sigma life science, St. Louis, MO, USA) and agar solidified media contained 1.5 % (w/v) agar (Lot #BCBV9964, G1296-1KG, Sigma life science).

The agar media used to assess the effect of Al on root growth was prepared by adjusting the pH to 5.5 with succinic acid, which was equal to the pH of the 0.8 % (w/v) gellan gum media (the pH of 1.5 % (w/v) agar media used for all other analyses was adjusted to 6.0).

Measurement of root elongation rate

Starting from 4 DAS, the level reached by the growing root tips was marked on the plate every day to record the position of the root tip of each seedling. This procedure was repeated until 10 DAS, at which point the plate was scanned and its digital image was saved. The distance between successive marks along the roots were determined from digitized images using ImageJ ver. 1.51m9 (NIH Image, Bethesda, MD, USA). Average root elongation rate was calculated each day as the measured distance of root tip movement divided by the corresponding time interval between markings (approximately 24 h).

Measurement of physico-chemical properties of the media

Water potential

The water potential of each medium was measured using a dewpoint potentiometer WP4C, Decagon Devices, Inc., Pullman, WA, USA). After sterilization of the media, 6 mL of each medium was dispensed into steel WP4C cups and allowed to solidify into agar and gellan gum at room temperature. These cups were used as the samples for water potential measurement. Each sample had six replicates.

Gel hardness

The hardness of each media was measured by rupture strength analysis using a creep meter (RE2-33005B, YAMADEN, Tokyo, Japan). After sterilization of the media, 6 mL of each medium was dispensed into petri dishes and allowed to solidify at room temperature to be used as samples for gel hardness measurements. Each sample had six replicates.

Elemental analysis

Agar (approximately 60 mg) and gellan gum samples (approximately 300 mg) were dried at 70 °C and digested using concentrated HNO_3. Elemental analysis was performed using inductively coupled plasma atomic emission spectroscopy (ICP-AES) (SPS 3500, SII NanoTechnology, Tokyo, Japan). Sample measurements were taken using five replicates for each of agar and gellan gum. The agar samples were diluted 10-fold for measurement of Na, and the gellan gum samples were diluted 40-fold for measurement of Ca, Mg, and Na.

Statistical analysis

The Bartlett test was conducted with the measurement datasets of root elongation rate in polyploid series on each date (Fig. II-2; Fig. II-4b; Fig. II-5). The analysis did not indicate homogeneity of variance in some measurement datasets, therefore I decided to conduct the Kruskal-Wallis test with all measurement datasets. The analysis showed significance in all measurement datasets ($p < 0.01$) and then the Steel-Dwass test was conducted.

The Bartlett test was also conducted with the measurement dataset of gel hardness in 0.8 % gellan gum, 1.0 % agar and 1.5 % agar (Table II-1). The

analysis did not indicate homogeneity of variance in this dataset, therefore we decided to conduct the Kruskal-Wallis test with this datasets. The analysis showed significance in this dataset ($p < 0.01$) and then the Steel-Dwass test was conducted.

The Welch's *t*-test was conducted with the measurement data of root elongation rate in 1.5 % agar medium with 0 μM and 30 gellan gum of polyploid series on each date (Fig. II-6), the measurement data of water potential in the 0.8 % gellan gum and 1.5 % agar media, the measurement data of water potential in the 1.5 % agar with 0 mM mannitol and 1.5 % agar with 20 mM mannitol (Table II-2), and the concentration of each element in agar and gellan gum media (Table II-3).

The Bartlett test and the Steel-Dwass test were conducted using the software R version 3.4.0 (R Development Core Team). The Kruskal-Wallis test and the Welch's *t*-test were conducted using the software KaleidaGraph version 5.0 (Synergy Software).

Results

Root elongation of seedlings of polyploid series grown on gellan gum and agar media

I observed the seedlings of polyploid series of *A. thaliana* and measured their root elongation rates on both gellan gum and agar media, which aims to characterize the effect of difference in gelling agent on polyploidy-dependent growth.

A comparison of the polyploid series of *A. thaliana* grown vertically on 0.8 % gellan gum and 1.5 % agar media at 10 DAS showed that gellan gum promoted the root growth of diploids whereas agar promoted the growth of polyploids (tetraploid, hexaploid, and octoploid) (Fig. II-1).

I measured the root elongation rates of polyploid series grown on 0.8 % gellan gum and 1.5 % agar media from 4 to 10 DAS (Fig. II-2a, b). When grown on 0.8 % gellan gum media, I observed a gradual reduction in root length of seedlings with increasing ploidy levels; root elongation rate of diploids was the highest (Fig. II-2a).

Contrasting results were obtained in the case of agar (Fig. II-2b). The root elongation rates of polyploids (tetraploid, hexaploid, and octoploid) grown on 1.5 % agar media were higher than those for polyploids grown on 0.8 % gellan gum media, while the root elongation rate of diploids was suppressed. Consequently, the root elongation rate of diploids was lower than that of tetraploids when grown on 1.5 % agar media.

The assessment of gel hardness of agar and gellan gum

I measured the gel hardness of several media changing the type and concentration of gelling agents. Then, I measured the root elongation rate of polyploid series grown on the agar medium with gel hardness adjusted to be softer than that of the 0.8 % gellan gum medium, which aims to determine the effects of gel hardness on the root elongation of polyploid series.

I measured the gel hardness of both gellan gum and agar media at several concentrations (Fig. II-3a). The gel hardness of both media increased proportionally with the concentration of the gelling agent. When compared at the

same concentration of the gelling agent, the gellan gum media was always harder than the agar media.

The gel hardness of 0.8 % gellan gum, 1.0 % agar, and 1.5 % agar media (Fig. II-3a) are listed in Table II-1. The gel hardness of 1.5 % agar medium was significantly higher than that of 0.8 % gellan gum medium, while that of 1.0 % agar medium was significantly lower than that of 0.8 % gellan gum medium (Table II-1).

Subsequently, I measured the root elongation rate of polyploids grown on 1.0 % (w/v) agar medium (Fig. II-2c). The root elongation rates of diploid, tetraploid, and hexaploid grown on the softer (1.0 %) agar medium at all measurement dates were more than those grown on the harder (1.5 %) agar media, while the root elongation rate of octoploid was almost the same on both media (Fig. II-2b, c).

The assessment of water potential of agar and gellan gum

I measured the water potentials of several media changing the type and concentration of gelling agents. Then, I measured the root elongation rate of the polyploid series grown on the agar medium with water potential adjusted to the almost same water potential in the 0.8 % gellan gum medium, which aims to determine the effects of water potential on the root elongation of polyploid series.

I measured the water potentials of gellan gum and agar media at several concentrations (Fig. II-3b). The lower the water potential, the lesser the water transferred from a medium to the roots. The water potential of the agar was almost constant at all concentrations, while that of the gellan gum decreased at

high concentrations. The water potential of the agar was higher than that of the gellan gum at all concentrations.

I added mannitol to the 1.5 % agar medium in several concentrations to reduce the water potential (Fig. II-4a). The water potential of the medium was almost constant at lower concentrations of mannitol (0, 5, 10 mM), but it decreased proportionally with the concentration of mannitol at higher concentrations (20, 50, 100 mM).

The water potentials of 0.8 % gellan gum and 1.5 % agar media (Fig. II-3b), and those of 1.5 % agar medium with 0 mM and 20 mM mannitol (Fig. II-4a) are listed in Table II-2. The addition of 20 mM mannitol to 1.5 % agar medium significantly decreased water potential. Water potential of agar medium with 20 mM mannitol was almost the same as that of 0.8 % gellan gum. Subsequently, I measured the root elongation rate of the polyploid series grown on agar media with 0 mM and 20 mM mannitol from 4 to 10 DAS (Fig. II-4b). The temporal profile of elongation rate on the agar medium with 0 mM mannitol was similar to that on the agar medium with 20 mM mannitol.

The assessment of trace elements of agar and gellan gum

I determined the amount of trace elements in each gelling agent to analyze their effects on the root elongation of polyploid series of *A. thaliana.* Then I determined a candidate element responsible for the change in polyploidy-dependent growth and examined its effects on the root elongation of polyploid series.

I quantified the concentrations of trace elements in 0.8 % gellan gum media and 1.5 % agar media using ICP-AES (Table II-3). Elemental analysis

showed that gellan gum contained significantly more magnesium (Mg), aluminum (Al), and calcium (Ca) than agar, whereas agar contained significantly more sodium (Na), iron (Fe), and cadmium (Cd) than gellan gum (Welch's *t*-test, $p < 0.05$). No significant differences were found in boron (B), titanium (Ti), and manganese (Mn) contents between the gelling agents. Chromium (Cr) and copper (Cu) were not detected in either gelling agent.

As Al has been widely considered to suppress the root elongation in *A. thaliana* (Koyama et al. 1994; Rounds and Larsen 2008; Sun et al. 2010; Yang et al. 2014; Sjogren et al. 2015), I focused on Al among all trace elements and added it to the agar medium and examined whether Al inhibits root elongation in polyploids. I measured the root elongation rate of the polyploid series grown on 1.5 % agar media supplemented with the same concentration of Al (30 μM) in the 0.8 % gellan gum media (Fig. II-5). The root elongation rate of diploids did not change significantly between the 1.5 % agar medium without additional Al and that with 30 μM Al (Fig. II-6a), while the root elongation rate of tetraploids significantly decreased from 4–5 DAS to 7–8 DAS (Fig. II-6b). The root elongation rate of octoploid significantly decreased from 6–7 DAS to 8–9 DAS (Fig. II-6d), whereas the root elongation rate of hexaploids did not decrease but significantly increased at 6–7 DAS (Fig. II-6c).

Discussion

Gellan gum and agar differently affect the change in root elongation by polyploidization

The measurement of root elongation rate in polyploid series grown on gellan gum and agar media (Fig. II-2) confirmed my preliminary observation that the change in growth due to polyploidization differs between the two gelling agents, as the components of each medium were identical except for the gelling agent. This is the first study to demonstrate that the type of gelling agent influences the polyploidization effect on plant growth.

Physical properties of gelling agents are not key factors affecting the difference in change in growth due to polyploidization

Nakagawa et al. (2007) revealed that the primary root of the wild type of *A. thaliana* could penetrate the harder layer of double-layer agar medium, whereas *mca1-null* mutant could not. As MCA1 is considered to be a Ca^{2+}-permeable stretch-activated (SA) channel (Yoshimura et al, 2021), the result of the experiment using double-layer agar medium suggests that the Ca^{2+}-permeable SA channel could detect the gel hardness and affect the root elongation of *A. thaliana*. Therefore, I expected that each polyploid might detect the gel hardness of the gellan gum and agar media differently, leading to differences in change in growth due to polyploidization between the two gelling agents (Fig. II-1, II-2).

However, the results suggest that the gel hardness was not a critical factor in determining the difference of change in growth by polyploidization (Fig. II-2). The root elongation rate in diploids, tetraploids, and hexaploids was promoted when they were grown on the softer agar medium (1.0 % agar) with a gel hardness similar to that of the 0.8 % gellan gum medium; however, the relationship among the temporal profiles of root elongation rate in polyploids was mostly unchanged compared with those grown on the normal agar medium

(1.5 % agar) (Fig. II-2b, c). Schultz et al. (2016) analyzed the root growth grown on three kinds of gelling agents and revealed that differences in media type had more of an impact on root growth than hardness itself, which is consistent with the results of this study.

The control of water potential in media is related to the control of water availability, and the water availability is directly related to the plant growth. In the roots of *A. thaliana*, the lower the water potential of medium was, the lower was the elongation rate (van der Weele et al. 2000). The results suggest that the water potential affects the root elongation rate and each polyploid may detect the water availability differently, leading to differences in change in growth due to polyploidization between gellan gum and agar.

However, the results of this study suggest that the water potential is not a critical factor in determining the difference in change in growth due to polyploidization (Fig. II-2, II-4). The temporal profiles of root elongation rate in polyploids in the normal 1.5 % agar medium (0 mM mannitol) and in the 1.5 % agar medium with the lower water potential (20 mM mannitol) are similar, which did not correspond to that of the 0.8 % gellan gum medium. In a previous study, a difference of water potential between each pair of growth conditions was at least more than 0.1 MPa (van der Weele et al. 2000); however, the difference of water potential between the 1.5 % agar medium + 0 mM mannitol and the 1.5 % agar medium + 20 mM mannitol was 0.05 MPa in this study (Table II-2), which may be too low to affect the change in growth due to polyploidization.

Aluminum in the gellan gum could partially explain the effects of agar and gellan gum on the root growth of polyploids

Quantitative analysis of trace elements in gellan gum and agar showed that the contents of some element differed significantly (Table II-3). Agar contained significantly higher Na, Fe, and Cd than gellan gum. In contrast, gellan gum contains significantly higher Mg, Al, and Ca. The root elongation of *A. thaliana* was usually suppressed by more than 10 mM NaCl in previous studies (West et al. 2004; Jiang et al. 2016; Zhao et al. 2017; Fu et al. 2019), and the contents of Na in gellan gum and agar were significantly lower than 10 mM in this study (ca 7.8 mM in gellan gum and 1.8 mM, Table II-3), which could not affect the root elongation because they are too low. The deficiency of Fe, Mg, and Ca in media severely suppressed the root elongation of *A. thaliana* (Gruber et al. 2013), but the 1/2 MS medium, which is the base medium used in this study, contains a large amount of Fe, Mg, and Ca (1500 μM Ca, 750 μM Mg and 45 μM Fe, Murashige and Skoog 1962). Therefore, the contents of Fe, Mg, and Ca in gellan gum and agar could not affect the root elongation (Table II-3). Cd is well known to suppress root elongation in plants (Godbold and Hüttermann 1985; Munzuroglu and Geckil 2004). However, less than 5 μM Cd did not severely suppressed the root elongation of *A. thaliana* (Wójcik and Tukiendorf 2004; Van Belleghem et al. 2007), which suggests that the contents of Cd in gellan gum and agar were too low to affect the root elongation (0.320 μM in agar and 0.028 μM in gellan gum, Table II-3).

On the other hand, Al significantly suppressed the root elongation of *A. thaliana* at 20 μM (Sun et al. 2010), 50 μM (Zhu et al. 2012), 6 μM (Yang et al. 2014). The content of Al in gellan gum was 33.401 μM (Table II-3), which is within the range of content that could suppress the root elongation of *A. thaliana*. Therefore, I focused on the effect of Al in gellan gum and conducted Al addition experiment in agar media for polyploids.

The results of Al addition experiment showed that the root elongation rate of tetraploids and octoploids grown on the 1.5 % agar medium with 30 μM Al was significantly suppressed, while that of diploids remained unchanged (Fig. II-6a, b, d). The root elongations of diploids and tetraploids were almost the same at 5–6, 6–7, and 7–8 DAS and the differences between the root elongations of diploids and tetraploids were relatively small at other measurement dates when grown on the 1.5 % agar medium with 30 μM Al, whereas the root elongation rate of tetraploids was significantly higher than that of diploids at all measurement dates when grown on the 1.5 % agar medium with no additional Al (0 μM Al) (Fig. II-5a, b). In addition, the root elongation of octoploid grown on the 1.5 % agar medium with 30 μM Al significantly decreased. These results suggest that the higher Al concentration in gellan gum could partially explain the differences in change in growth due to polyploidization between 0.8 % gellan gum and 1.5 % agar medium. As the root elongation rate of diploids was significantly higher than that of tetraploids grown on the 0.8 % gellan gum medium, the addition of Al to the agar medium did not completely reproduce the relationship of temporal profiles in root elongation between diploids and tetraploids grown on the 0.8 % gellan gum medium. The relationship between diploids and tetraploids grown on the agar medium with 30 μM Al, however, is closer to that of those grown on the 0.8 % gellan gum medium than that of those grown on the agar medium with 0 μM Al, which suggests that the decrease in root elongation of tetraploid in the 0.8 % gellan gum medium should be partially attributed to the Al in gellan gum (Fig. II-2, II-5).

Al binds to cell wall components, especially hemicellulose, thereby reducing cell wall extensibility and inhibiting root elongation (Yang et al. 2011). Polyploids of *A. thaliana* have been shown to have an increased amount of

hemicellulose compared with diploid plants (Corneillie et al., 2019), which may have contributed to the tetraploids and octoploids being more sensitive to Al than diploid in root elongation rate.

The root elongation rate of hexaploids grown on the 1.5 % agar medium with 30 μM Al was similar to that of those grown on the 1.5 % agar medium with 0 μM Al. However, further studies are needed to understand as to why the addition of Al did not have any effect on the root elongation of hexaploids, while it suppressed those of tetraploids and octoploids.

This study is the first report of the different effects of two major gelling agents, gellan gum and agar, on change in growth due to polyploidization. My findings indicate that Al, which is more abundant in gellan gum, suppresses root elongation in tetraploids and octoploids, which could be partly attributed to the different effects of gellan gum and agar on the change in growth due to polyploidization. However, the physical properties of gellan gum and agar media, gel hardness, and water potential, may not be responsible for these effects.

Concluding remarks

In Chapter II, I analyzed the effect of gelling agents (agar and gellan gum) as environmental factors on growth changes caused by polyploidization. The physical properties (gel hardness and water potential) and chemical properties (trace element contents) of agar and gellan gum media were examined. Further, I investigated the relationship between these media properties and the root elongation rate of the polyploid series of *A. thaliana*. For the gel hardness of the medium, the harder the medium, the more suppressed is the root elongation in all polyploid strains. For the water potential of the medium, the gellan gum medium

had a lower water potential than that of the agar medium. Mannitol was then added to the agar medium to reduce the water potential to the same level as that of the gellan gum medium. However, there was no significant change in each polyploid strain's root elongation rate grown on agar medium containing mannitol. Based on these results, the media's gel hardness and water potential were not related to the promotion of root elongation in polyploids grown on the agar medium. I subsequently measured the trace elements in the gelling agents and observed that gellan gum contained more aluminum than agar. Because aluminum suppresses root tip elongation, I grew the polyploid series on agar medium with the same amount of aluminum as the gellan gum medium and measured the root elongation rate. The results revealed that the root elongation rate of tetraploids and octoploids was suppressed when grown on the medium with added aluminum compared to the medium without aluminum. Based on these results, aluminum, which is abundant in gellan gum, partially contributes to suppressing the root elongation of polyploids when grown on a gellan gum medium.

Table II-1. Gel hardness of medium

medium	gel hardness (N)			
0.8% gellan gum	1.23	±	0.03	a
1.0% agar	1.03	±	0.03	b
1.5% agar	1.86	±	0.08	c

Data shows mean ± standard errors (n = 6). All data were taken from Fig. II-3a. Different alphabets indicate significant difference between media at $p < 0.05$ (Steel-Dwass test)

Table II-2. Water potential of medium

medium	water potential (MPa)			
0.8% gellan gum	-0.25	±	0.01	*
1.5% agar	-0.21	±	0.01	
1.5% agar + 0 mM mannitol	-0.22	±	0.01	**
1.5% agar + 20 mM mannitol	-0.27	±	0.01	

Data shows mean ± standard errors (n = 6). Data of 0.8% gellan gum and 1.5% agar media were taken from Fig. II-3b, and data of 1.5% agar medium + 0 mM and 20 mM mannitol were taken from Fig. II-4a. * indicates statistical difference (Welch' s t test. *$0.01<p<0.05$, **$p<0.01$)

Table II-3. Elemental analysis of gelling agents

Element	Agar		Gellan gum		p-value	
B	154	± 66	9.88	± 9.80	0.094	
Na	7802	± 184	1830	± 244	< 0.0001	*
Mg	139	± 2	260	± 33	0.021	*
Al	2.523	± 1.690	33.4	± 4.2	0.0009	*
Ca	166	± 3	439	± 55	0.0076	*
Ti	1.97	± 0.76	0.0552	± 0.0195	0.065	
Cr	n. d.		n. d.			
Mn	0.689	± 0.0357	0.776	± 0.099	0.44	
Fe	18.07	± 1.74	7.40	± 0.92	0.0016	*
Cu	n. d.		n. d.			
Cd	0.319	± 0.017	0.0281	± 0.00151	< 0.0001	*

Data shows mean (μM) ± standard deviation (n = 5). *Indicates significant difference between agar and gellan gum at $p < 0.05$ (Welch's t test). n.d. indicates not detected

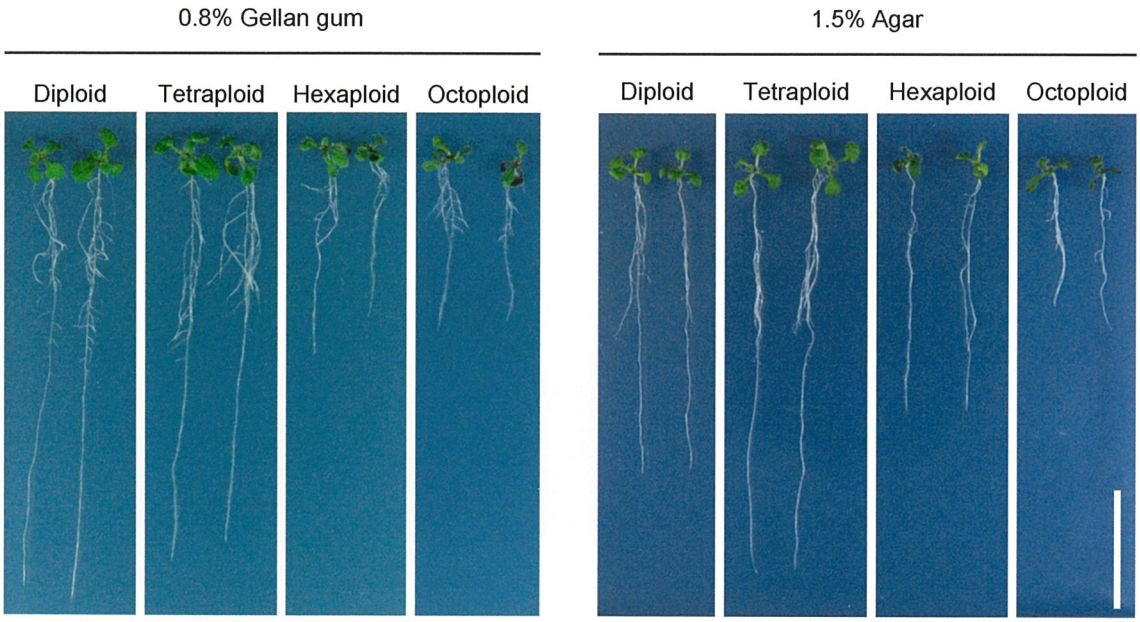

Figure II-1. Different effects of gellan gum and agar on root growth of polyploid series in *Arabidopsis thaliana*

10-day-old seedlings grown vertically on MS medium solidified by gellan gum or agar. Scale bar = 2 cm

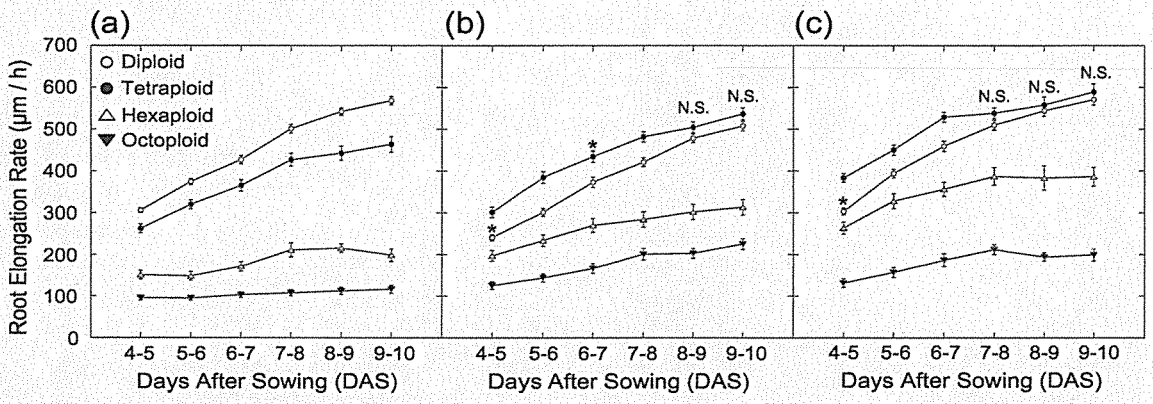

Figure II-2. Root elongation rate of polyploid series grown on gellan gum or agar medium

(a) Cultured on 0.8 % (w/v) gellan gum medium. n = 38 (diploid), 40 (tetraploid), 23 (hexaploid), 39 (octoploid). A significant difference in the root elongation rate was observed between every pair grown on gellan gum media for all days from 4–5 DAS to 9–10 DAS (Steel-Dwass test, $p < 0.01$). (b) Cultured on 1.5 % (w/v) agar medium. n = 33 (diploid), 33 (tetraploid), 22 (hexaploid), 26 (octoploid). There was a significant difference in the root elongation rate between every pair grown on agar media for all days from 4–5 DAS to 9–10 DAS (Steel-Dwass test, $p < 0.01$), except between diploid and tetraploid pairs for 6–7 DAS (*, Steel-Dwass test, $0.01 < p < 0.05$) , 8–9 DAS and 9–10 DAS (N.S., Steel-Dwass test, $0.05< p$), and tetraploid and hexaploid pairs for 4–5 DAS (*, Steel-Dwass test, $0.01 < p < 0.05$). (c) Cultured on 1.0 % (w/v) agar (softer) medium. n = 42 (diploid), 35 (tetraploid), 20 (hexaploid), 23 (octoploid). There was a significant difference in the root elongation rate between every pair grown on agar media for all days from 4–5 DAS to 9–10 DAS (Steel-Dwass test, $p < 0.01$), except between diploid and tetraploid pairs for 7–8 DAS to 9–10 DAS (N.S., Steel-Dwass test, $0.05 < p$), and tetraploid and hexaploid pairs for 4–5 DAS (*, Steel-Dwass test, $0.01 < p < 0.05$). Bars indicate standard errors

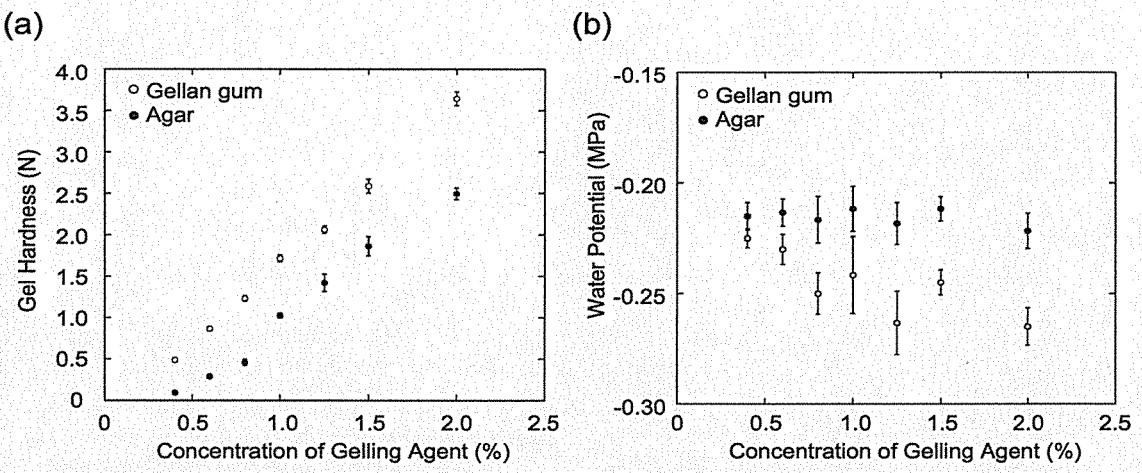

Figure II-3. Relationship between concentration of gelling agent and physical properties (gel hardness and water potential)

(a) Gel hardness. n = 6 for each data point. Bars indicate standard errors. (b) Water potential. n = 6 for each data point. Bars indicate standard errors

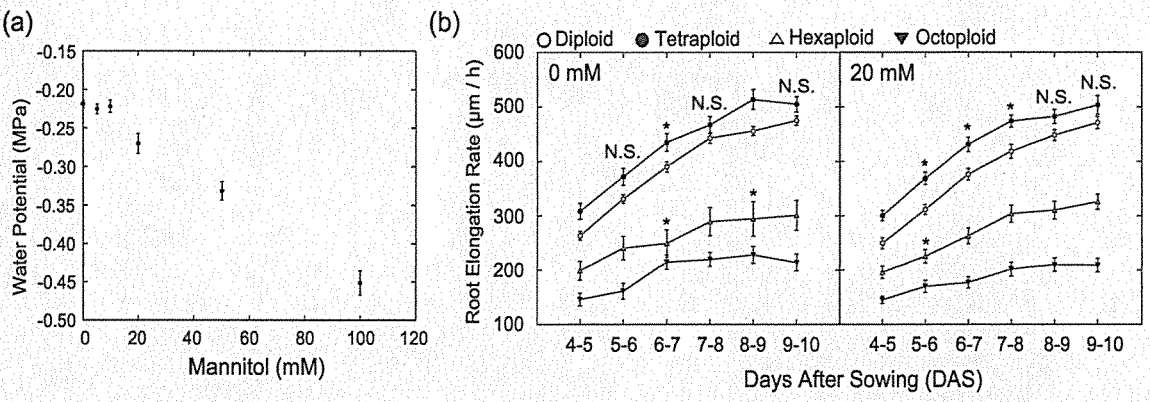

Figure II-4. Relationship between water potential and root elongation rate on agar media

(a) Water potential of 1.5 % agar medium with mannitol at several concentrations (0, 5, 10, 20, 50, 100 mM). n = 6 for each data point. Bars indicate standard errors. (b) Root elongation rate. Cultured on 1.5 % agar medium with 0 or 20 mM mannitol. n = 32 (0 mM, diploid), 26 (0 mM, tetraploid), 18, (0 mM, hexaploid), 16 (0 mM, octoploid), 26 (20 mM, diploid), 20 (20 mM, tetraploid), 25, (20 mM, hexaploid), 40 (20 mM, octoploid). There was a significant difference in the root elongation rate between every pair grown on agar media for all days from 4–5 DAS to 9–10 DAS (Steel-Dwass test, $p < 0.01$), except between diploid and tetraploid pairs for 5–6 DAS, 7-8 DAS, and 9–10 DAS in 0 mM mannitol medium and 8-9 DAS and 9–10 DAS in 20 mM mannitol medium (N.S., Steel-Dwass test, $0.05 < p$), diploid and tetraploid pairs for 6-7 DAS in 0 mM mannitol medium and 5-6 DAS to 7-8 DAS in 20 mM mannitol medium (*, Steel-Dwass test, $0.01 < p < 0.05$), and hexaploid and octoploid pairs for 6–7 DAS and 8-9 DAS in 0 mM mannitol medium and 5-6 DAS in 20 mM mannitol medium (*, Steel-Dwass test, $0.01 < p < 0.05$). Bars indicate standard errors

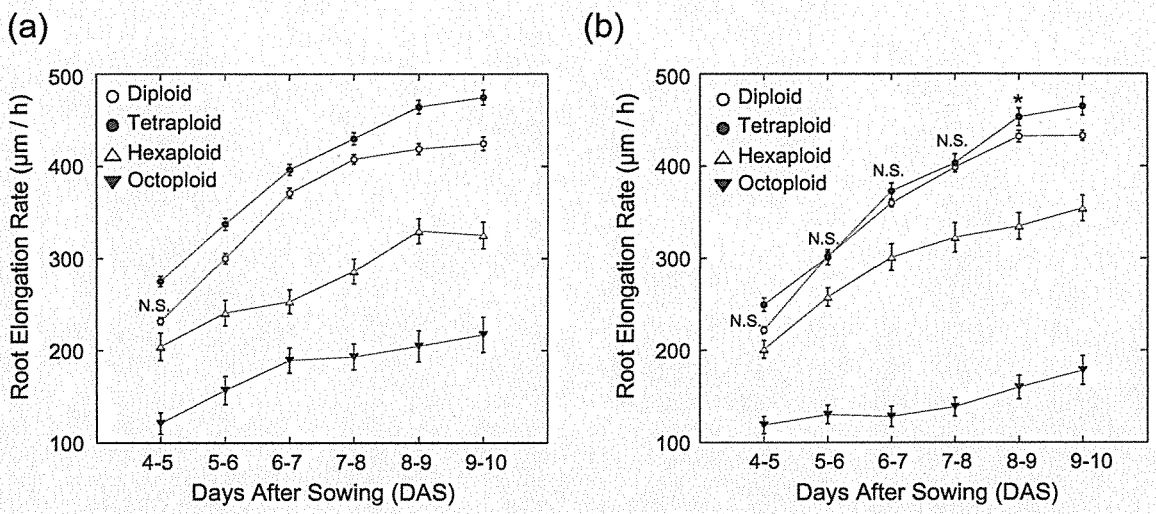

Figure II-5. Effect of aluminum on root elongation rate of polyploid series on agar media

(a) Cultured on 1.5 % agar medium with 0 μM Al. n = 74 (diploid), 70 (tetraploid), 23 (hexaploid), 20 (octoploid). (b) Cultured on 1.5 % agar medium with 30 μM Al medium. n = 74 (diploid), 54 (tetraploid), 27 (hexaploid), 16 (octoploid). There was a significant difference in the root elongation rate between every pair grown on agar media for all days from 4–5 DAS to 9–10 DAS (Steel-Dwass test, $p < 0.01$), except between diploid and tetraploid pairs for 5–6 DAS to 7–8 DAS (N.S., Steel-Dwass test, $0.05 < p$) and 8-9 DAS (*, Steel-Dwass test, $0.01 < p < 0.05$) in (b), and tetraploid and hexaploid pairs for 4–5 DAS (N.S., Steel-Dwass test, $0.05 < p$) in (a) and (b). Bars indicate standard errors

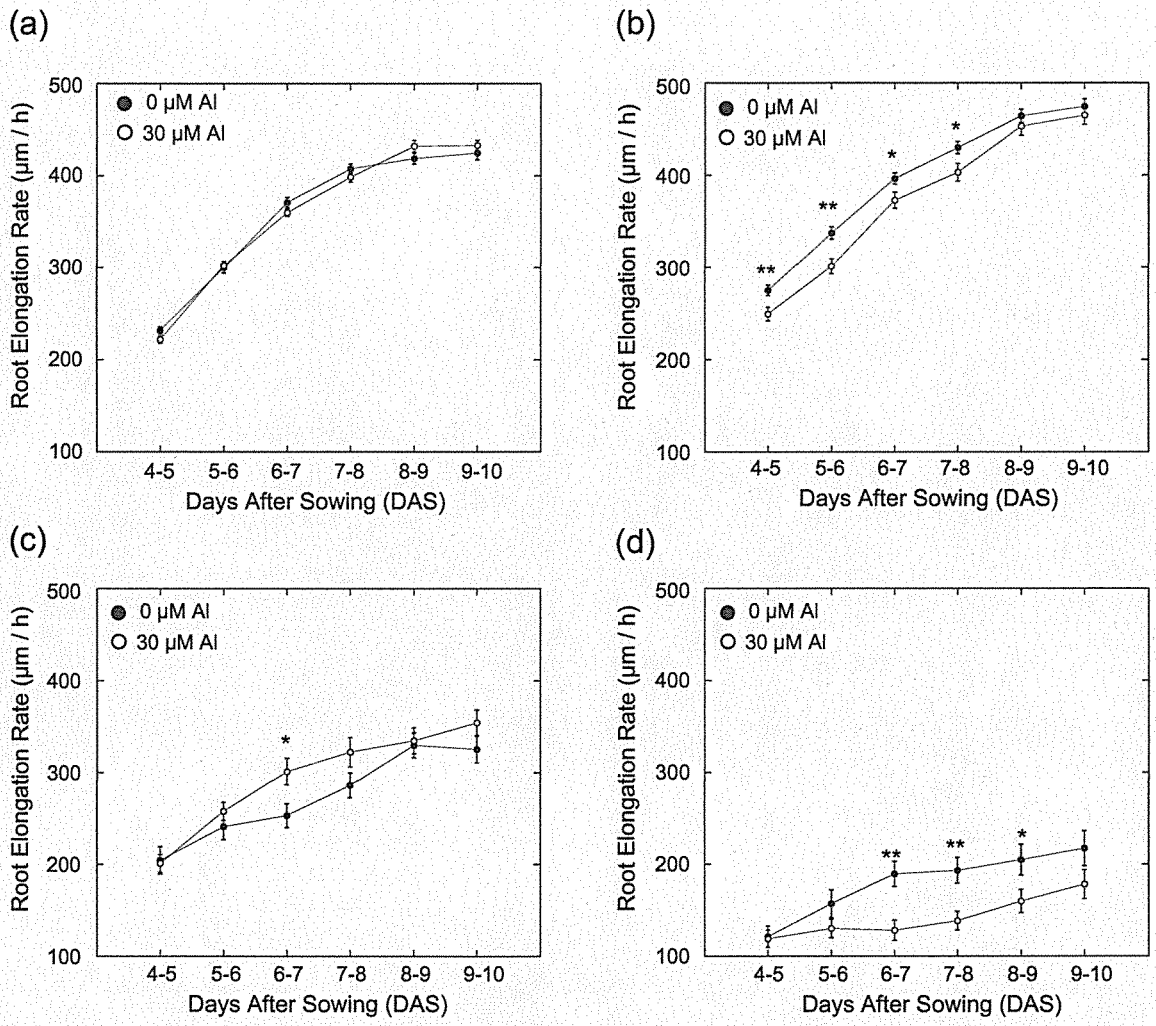

Figure II-6. The effect of aluminum on the root elongation rate of the polyploids Raw data shown in Fig. II-5 were used.

(a) Diploid. n = 74 (0 μM), 74 (30 μM), (b) Tetraploid. n = 70 (0 μM), 54 (30 μM), (c) Hexaploid. n = 23 (0 μM), 27 (30 μM), (d) Octoploid. n = 20 (0 μM), 16 (30 μM). * Indicates statistical difference (Welch' s *t*-test. *$0.01<p<0.05$, **$p<0.01$). Bars indicate standard errors

References

Al-Mayahi AMW, Ali AH (2021) Effects of different types of gelling agents on in vitro organogenesis and some physicochemical properties of date palm buds, Showathy cv. *Folia Oecologica* **48**:110–117. https://doi.org/10.2478/foecol-2021-0012

Berger K, Schaffner W (1995) In vitro propagation of the leguminous tree *Swartzia madagascariensis*. *Plant Cell, Tissue and Organ Culture* **40**:289–291. https://doi.org/10.1007/BF00048136

Buah JN, Kawamitsu Y, Sato S, Murayama S (1999) Effects of different types and concentrations of gelling agents on the physical and chemical properties of media and the growth of Banana (*Musa* spp.) *in vitro*. *Plant Production Science* **2**:138–145. https://doi.org/10.1626/pps.2.138

Corneillie S, De Storme N, Van Acker R, Fangel JU, De Bruyne M, De Rycke R, Geelen D, Willats WGT, Vanholme B, Boerjan W (2019) Polyploidy affects plant growth and alters cell wall composition. *Plant Physiology* **179**:74–87. https://doi.org/10.1104/pp.18.00967

Debergh PC (1983) Effects of agar brand and concentration on the tissue culture medium. Physiologia Plantarum **59**:270–276. https://doi.org/10.1111/j.1399-3054.1983.tb00770.x

Fatima A, Khan SJ (2011) Some factors affecting the *in vitro* growth of *Stevia rebaudiana* Bertoni. *Iranian Journal of Plant Physiology* **1**:61–68.

Fu Y, Yang Y, Chen S, Ning N, Hu H (2019) Arabidopsis IAR4 modulates primary root growth under salt stress through ROS-mediated modulation of auxin distribution. *Frontiers in plant science* **10**:522. https://doi.org/10.3389/fpls.2019.00522

Godbold DL, Hüttermann A (1985) Effect of zinc, cadmium and mercury on root elongation of *Picea abies* (Karst.) seedlings, and the significance of these metals to forest die-back. *Environmental Pollution Series A, Ecological and Biological* **38**:375–381. https://doi.org/10.1016/0143-1471(85)90108-4

Gruber BD, Giehl RFH, Friedel S, von Wirén N (2013) Plasticity of the Arabidopsis root system under nutrient deficiencies. *Plant Physiology* **163**:161–179. https://doi.org/10.1104/pp.113.218453

Ichi T, Koda T, Asai I, Hatanaka A, Sekiya J (1986) Effects of gelling agents on *in vitro* culture of plant tissues. *Agricultural and Biological Chemistry* **50**:2397–2399. https://doi.org/10.1080/00021369.1986.10867756

Ichimura K, Oda M (1998) Stimulation of root growth of several vegetables by extracts from a commercial preparation of agar. *Journal of the Japanese Society for Horticultural Science* **67**:341–346. https://doi.org/10.2503/jjshs.67.341

Iwamoto A, Kondo E, Fujihashi H, Sugiyama M (2013) Kinematic study of root elongation in *Arabidopsis thaliana* with a novel image-analysis program. *Journal of Plant Research* **126**:187–192. https://doi.org/10.1007/s10265-012-0523-5

Iwamoto A, Satoh D, Furutani M, Maruyama S, Ohba H, Sugiyama M (2006) Insight into the basis of root growth in *Arabidopsis thaliana* provided by a simple mathematical model. *Journal of plant research* **119**:85–93. https://doi.org/10.1007/s10265-005-0247-x

Jacques CN, Hulbert AK, Westenskow S, Neff MM (2020) Production location of the gelling agent Phytagel has a significant impact on *Arabidopsis thaliana* seedling phenotypic analysis. *PLOS ONE* **15**:e0228515. https://doi.org/10.1371/journal.pone.0228515

Jansson P-E, Lindberg B, Sandford PA (1983) Structural studies of gellan gum, an extracellular polysaccharide elaborated by *Pseudomonas elodea*. *Carbohydrate Research* **124**:135–139. https://doi.org/10.1016/0008-6215(83)88361-X

Jiang K, Moe-Lange J, Hennet L, Feldman LJ (2016) Salt stress affects the redox status of *Arabidopsis* root meristems. *Frontiers in Plant Science* **7**:81–90. https://doi.org/10.3389/fpls.2016.00081

Johnston JS, Bennett MD, Rayburn AL, Galbraith DW, Price HJ (1999) Reference standards for determination of DNA content of plant nuclei. *American Journal of Botany* **86**:609–613. https://doi.org/10.2307/2656569

Kikuchi S, Iwamoto A (2020) Quantitative analysis of chromosome polytenization in synthetic autopolyploids of *Arabidopsis thaliana*. *Cytologia* **85**:189–195. https://doi.org/10.1508/cytologia.85.189

Kikuchi S, Iwamoto A (2021) An efficient method of tetraploid and octaploid induction in *Arabidopsis thaliana* using colchicine treatment. *Science Journal of Kanagawa University* **32**:81–86.

Kirchmajer DM, Steinhoff B, Warren H, Clark R, in het Panhuis M (2014) Enhanced gelation properties of purified gellan gum. *Carbohydrate Research* **388**:125–129. https://doi.org/10.1016/j.carres.2014.02.018

Klimaszewska K, bernier-Cardou M, Cyr DR, Sutton BCS (2000) Influence of gelling agents on culture medium gel strength, water availability, tissue water potential, and maturation response in embryogenic cultures of *Pinus strobus* L. *In Vitro Cellular & Developmental Biology - Plant* **36**:279–286. https://doi.org/10.1007/s11627-000-0051-1

Koyama H, Toda T, Yokota S, Dawair Z, Hara T (1994) Effects of aluminum and pH on root growth and cell viability in *Arabidopsis thaliana* strain Landsberg

in hydroponic culture. *Plant and Cell Physiology* **36**:201–205. https://doi.org/10.1093/oxfordjournals.pcp.a078740

Kumar N, Reddy MP (2011) In vitro plant propagation: a review. *Journal of Forest and Environmental Science* **27**:61–72. https://doi.org/10.7747/JFS.2011.27.2.1

Leitch IJ, Bennett MD (1997) Polyploidy in angiosperms. *Trends in plant science* **2**:470–476. https://doi.org/10.1016/S1360-1385(97)01154-0

Levin DA (1983) Polyploidy and novelty in flowering plants. *The American Naturalist* **122**:1–25. https://doi.org/10.1086/284115

Masondo NA, Aremu AO, Finnie JF, Van Staden J (2015) Growth and phytochemical levels in micropropagated *Eucomis autumnalis* subspecies *autumnalis* using different gelling agents, explant source, and plant growth regulators. *In Vitro Cellular & Developmental Biology - Plant* **51**:102–110. https://doi.org/10.1007/s11627-014-9646-9

Mitić N, Stanišić M, Milojević J, Tubić L, Ćosić T, Nikolić R, Ninković S, Miletić R (2012) Optimization of *in vitro* regeneration from leaf explants of apple cultivars Golden Delicious and Melrose. *American Society for Horticultural Science* **47**:1117–1122. https://doi.org/10.21273/HORTSCI.47.8.1117

Morris ER, Nishinari K, Rinaudo M (2012) Gelation of gellan – a review. *Food Hydrocolloids* **28**:373–411. https://doi.org/10.1016/j.foodhyd.2012.01.004

Munzuroglu O, Geckil H (2002) Effects of metals on seed germination, root elongation, and coleoptile and hypocotyl growth in *Triticum aestivum* and *Cucumis sativus*. *Archives of Environmental Contamination and Toxicology* **43**:203–213. https://doi.org/10.1007/s00244-002-1116-4

Murashige T, Skoog F (1962) A revised medium for rapid growth and bio assays with tobacco tissue cultures. *Physiologia Plantarum* **15**:473–497. https://doi.org/10.1111/j.1399-3054.1962.tb08052.x

Nakagawa Y, Katagiri T, Shinozaki K, Qi Z, Tatsumi H, Furuichi T, Kishigami A, Sokabe M, Kojima I, Sato S (2007) *Arabidopsis* plasma membrane protein crucial for Ca^{2+} influx and touch sensing in roots. *Proceedings of the National Academy of Sciences* **104**:3639–3644. https://doi.org/10.1073/pnas.0607703104

Robinson DO, Coate JE, Singh A, Hong L, Bush M, Doyle JJ, Roeder AHK (2018) Ploidy and size at multiple scales in the Arabidopsis sepal. *The Plant Cell* **30**:2308–2329. https://doi.org/10.1105/tpc.18.00344

Rounds MA, Larsen PB (2008) Aluminum-dependent root-growth inhibition in *Arabidopsis* results from AtATR-regulated cell-cycle arrest. *Current Biology* **18**:1495–1500. https://doi.org/10.1016/j.cub.2008.08.050

Schultz ER, Paul A-L, Ferl RJ (2016) Root growth patterns and morphometric change based on the growth media. *Microgravity Science and Technology* **28**:621–631. https://doi.org/10.1007/s12217-016-9514-9

Sjogren CA, Bolaris SC, Larsen PB (2015) Aluminum-dependent terminal differentiation of the Arabidopsis root tip is mediated through an ATR-, ALT2-, and SOG1-regulated transcriptional response. *The Plant Cell* **27**:2501–2515. https://doi.org/10.1105/tpc.15.00172

Soltis DE, Soltis PS, Tate JA (2003) Advances in the study of polyploidy since plant speciation. *New Phytologist* **161**:173–191. https://doi.org/10.1046/j.1469-8137.2003.00948.x

Sun P, Tian Q-Y, Chen J, Zhang W-H (2010) Aluminium-induced inhibition of root elongation in *Arabidopsis* is mediated by ethylene and auxin. *Journal of Experimental Botany* **61**:347–356. https://doi.org/10.1093/jxb/erp306

Tsay H-S, Lee C-Y, Agrawal DC, Basker S (2006) Influence of ventilation closure, gelling agent and explant type on shoot bud proliferation and hyperhydricity in *Scrophularia yoshimurae*—a medicinal plant. *In Vitro Cellular & Developmental Biology - Plant* **42**:445–449. https://doi.org/10.1079/IVP2006791

Tsukaya H (2008) Controlling size in multicellular organs: focus on the leaf. *PLoS Biology* **6**:e174. https://doi.org/10.1371/journal.pbio.0060174

Usov AI (2011) Chapter 4 - Polysaccharides of the red algae. In: Horton D (ed) *Advances in Carbohydrate Chemistry and Biochemistry* pp 115–217.

Van Belleghem F, Cuypers A, Semane B, Smeets K, Vangronsveld J, d'Haen J, Valcke R (2007) Subcellular localization of cadmium in roots and leaves of *Arabidopsis thaliana*. *New Phytologist* **173**:495–508. https://doi.org/10.1111/j.1469-8137.2006.01940.x

van der Weele CM, Spollen WG, Sharp RE, Baskin TI (2000) Growth of *Arabidopsis thaliana* seedlings under water deficit studied by control of water potential in nutrient-agar media. *Journal of Experimental Botany* **51**:1555–1562. https://doi.org/10.1093/jexbot/51.350.1555

West G, Inze D, Beemster GTS (2004) Cell cycle modulation in the response of the primary root of Arabidopsis to salt stress. *Plant Physiology* **135**:1050–1058. https://doi.org/10.1104/pp.104.040022

Williams RR, Taji AM (1987) Effects of temperature, darkness and gelling agent on long-term storage of in vitro shoot cultures of Australian woody plant

species. *Plant Cell, Tissue and Organ Culture* **11**:151–156. https://doi.org/10.1007/BF00041848

Wójcik M, Tukiendorf A (2004) Phytochelatin synthesis and cadmium localization in wild type of *Arabidopsis thaliana*. *Plant Growth Regulation* **44**:71–80. https://doi.org/10.1007/s10725-004-1592-9

Yang JL, Zhu XF, Peng YX, Zheng C, Li GX, Liu Y, Shi YZ, Zheng SJ (2011) Cell wall hemicellulose contributes significantly to aluminum adsorption and root growth in Arabidopsis. *Plant Physiology* **155**:1885–1892. https://doi.org/10.1104/pp.111.172221

Yang Z-B, Geng X, He C, Zhang F, Wang R, Horst WJ, Ding Z (2014) TAA1-regulated local auxin biosynthesis in the root-apex transition zone mediates the aluminum-induced inhibition of root growth in *Arabidopsis*. *The Plant Cell* **26**:2889–2904. https://doi.org/10.1105/tpc.114.127993

Yoshimura K, Iida K, Iida H (2021) MCAs in Arabidopsis are Ca^{2+}-permeable mechanosensitive channels inherently sensitive to membrane tension. *Nature Communications* **12**:6074. https://doi.org/10.1038/s41467-021-26363-z

Zhao WT, Feng SJ, Li H, Faust F, Kleine T, Li LN, Yang ZM (2017) Salt stress-induced FERROCHELATASE 1 improves resistance to salt stress by limiting sodium accumulation in *Arabidopsis thaliana*. *Scientific Reports* **7**:14737. https://doi.org/10.1038/s41598-017-13593-9

Zhu XF, Shi YZ, Lei GJ, Fry SC, Zhang BC, Zhou YH, Braam J, Jiang T, Xu XY, Mao CZ, Pan YJ, Yang JL, Wu P, Zheng SJ (2012) XTH31, encoding an in vitro XEH/XET-active enzyme, regulates aluminum sensitivity by modulating in vivo XET action, cell wall xyloglucan content, and aluminum binding capacity in *Arabidopsis*. *The Plant Cell* **24**:4731–4747. https://doi.org/10.1105/tpc.112.106039

General discussion

Polyploidization is a major driving force for angiosperms speciation (Soltis et al. 2003; Leitch and Leitch 2008; Jiao et al. 2011; Scarpino et al. 2014; Van de Peer et al. 2021). Polyploids are believed to be more adaptive than their diploid progenitors because polyploidization often increases resistance to pathogens and environmental stress (Grant 1981; Levin 1983; te Beest et al. 2012; Islam et al. 2022). On the other hand, it has been reported that high-polyploids suppress plant growth, called as "high-ploidy syndrome" (Tsukaya, 2008; Kikuchi and Iwamoto, 2020).

I demonstrated that the high-ploidy syndrome exists in the high-autopolyploids (hexaploids and octoploids) of *A. thaliana* where cell volume increase was significantly suppressed, and the suppression of endoreduplication, chromosome polytenization, and the difference in response to aluminum stress caused the syndrome. In addition, I revealed that cell proliferation was suppressed in high-polyploids and tetraploids. This is the first report on the maladaptive effects of autopolyploidization and its mechanism. Changes in the chromosome structure and environmental factors can suppress organ growth in autopolyploids.

These findings suggest that plant speciation involves polyploidy. Some studies estimate that the abundance of autopolyploids in angiosperms should be the same as that of allopolyploids (Ramsey and Schemske 1998; Barker et al. 2016); however, others estimate that allopolyploids are more abundant than autopolyploid (Doyle and Sherman- Broyles 2017). It is still controversial which type of polyploid has promoted speciation and prevailed in angiosperms. This study may settle a long-term debate. Autopolyploids are more disadvantageous

than allopolyploids because of their maladaptive effects on organ growth, and the hybridization effects of allopolyploidization may counteract the growth suppression effects of autopolyploidization. In future studies, I will conduct a root growth analysis on *A. suecica,* which originated from hybridization between the majorly diploid *A. thaliana* and the majorly autotetraploid *A. arenosa* (Jakobsson et al., 2006; O'Kane et al., 1996) and compare its spatial profile of growth parameters with those of the autopolyploid series of *A. thaliana* to confirm whether the high-polyploid syndrome exists even in allopolyploid. In addition, I will observe the degree of endoreduplication, chromosome polytenization, and response to aluminum stress in the root growth of *A. arenosa* and examine the hypothesis that the hybridization effects of allopolyploidization counteract the growth suppression effects of autopolyploidization.

In contrast, several studies have reported that natural high-autopolyploids are more adaptive than diploids (Moreyra et al., 2021; Fernández et al. 2022). In these naturally high-autopolyploids, it is possible that the high-ploidy syndrome is overcome in some way, such as through suppression of chromosome polytenization. It is also important to observe the degree of endoreduplication, chromosome polytenization, and response to aluminum stress in the root growth of these species and to elucidate how they overcome the high-ploidy syndrome.

In this study, I elucidated the effects of autopolyploidization on the root growth of *A. thaliana* and its mechanisms. The results of this study provided new insights into the speciation of angiosperms driven by polyploidization.

References

Barker MS, Arrigo N, Baniaga AE, Li Z, Levin DA (2016) On the relative abundance of autopolyploids and allopolyploids. *New Phytologist* **210**:391–398. https://doi.org/10.1111/nph.13698

Doyle JJ, Sherman-Broyles S (2017) Double trouble: taxonomy and definitions of polyploidy. *New Phytologist* **213**:487–493

Fernández P, Hidalgo O, Juan A, Leitch IJ, Leitch AR, Palazzesi L, Pegoraro L, Viruel J, Pellicer J (2022) Genome insights into autopolyploid evolution: A case study in *Senecio doronicum* (Asteraceae) from the southern alps. *Plants* **11**:1235. https://doi.org/10.3390/plants11091235

Grant V (1981) Plant Speciation. *Columbia University Press*. https://doi.org/10.7312/gran92318

Islam MM, Deepo DM, Nasif SO, Siddique AB, Hassan O, Siddique AB, Paul NC (2022) Cytogenetics and consequences of polyploidization on different biotic-abiotic stress tolerance and the potential mechanisms involved. *Plants* **11**:2684. https://doi.org/10.3390/plants11202684

Jakobsson M, Hagenblad J, Tavaré S, Säll T, Halldén C, Lind-Halldén C, Nordborg M (2006) A unique recent origin of the allotetraploid species *Arabidopsis suecica*: Evidence from nuclear DNA markers. *Molecular Biology and Evolution* **23**:1217–1231. https://doi.org/10.1093/molbev/msk006

Jiao Y, Wickett NJ, Ayyampalayam S, Chanderbali AS, Landherr L, Ralph PE, Tomsho LP, Hu Y, Liang H, Soltis PS (2011) Ancestral polyploidy in seed plants and angiosperms. *Nature* **473**:97. https://doi.org/10.1038/nature09916

Kikuchi S, Iwamoto A (2020) Quantitative analysis of chromosome

polytenization in synthetic autopolyploids of *Arabidopsis thaliana*. *Cytologia* **85**:189–195. https://doi.org/10.1508/cytologia.85.189

Leitch AR, Leitch IJ (2008) Genomic plasticity and the diversity of polyploid plants. *Science* **320**:481–483. https://doi.org/10.1126/science.1153585

Levin DA (1983) Polyploidy and novelty in flowering plants. *The American Naturalist* **122**:1–25. https://doi.org/10.1086/284115

Moreyra LD, Márquez F, Susanna A, Garcia-Jacas N, Vázquez FM, López-Pujol J (2021) Genesis, evolution, and genetic diversity of the hexaploid, narrow endemic *Centaurea tentudaica*. *Diversity* **13**:72. https://doi.org/10.3390/d13020072

O'Kane SL, Schaal BA, Al-Shehbaz IA (1996) The origins of *Arabidopsis suecica* (Brassicaceae) as indicated by nuclear rDNA sequences. *Systematic Botany* **21**:559–566. https://doi.org/10.2307/2419615

Ramsey J, Schemske DW (1998) Pathways, mechanisms, and rates of polyploid formation in flowering plants. *Annual Review of Ecology and Systematics* **29**:467–501. https://doi.org/10.1146/annurev.ecolsys.29.1.467

Scarpino SV, Levin DA, Meyers LA (2014) Polyploid formation shapes flowering plant diversity. *The American Naturalist* **184**:456–465. https://doi.org/10.1086/677752

Soltis DE, Soltis PS, Tate JA (2003) Advances in the study of polyploidy since Plant speciation. *New Phytologist* **161**:173–191. https://doi.org/10.1046/j.1469-8137.2003.00948.x

te Beest M, Le Roux JJ, Richardson DM, Brysting AK, Suda J, Kubešová M, Pyšek P (2012) The more the better? The role of polyploidy in facilitating plant invasions. *Annals of Botany* **109**:19–45. https://doi.org/10.1093/aob/mcr277

Tsukaya H (2008) Controlling size in multicellular organs: focus on the leaf. *PLoS Biology* **6**:e174. https://doi.org/10.1371/journal.pbio.0060174

Van de Peer Y, Ashman T-L, Soltis PS, Soltis DE (2021) Polyploidy: an evolutionary and ecological force in stressful times. *The Plant Cell* **33**:11–26. https://doi.org/10.1093/plcell/koaa015

Acknowledgments

First, I would like to express my sincere gratitude to my supervisor, professor Akitoshi Iwamoto, for his continuous support and guidance. I would also like to express my appreciation to my advisors, Professors Kazuhito Inoue, Yoshitaka Azumi, and Kazuhiko Nishitani, for their constructive suggestions.

In addition, a special thanks to the following who provided valuable technical support. I would like to thank Professor Munetaka Sugiyama and Doctor Natsumaro Kutsuna for their contribution in conducting the kinematic analysis on a cellular basis. I have had excellent technical support from Lecturer Takuya Sakamoto and Professor Sachihiro Matsunaga for establishing a novel whole-mount FISH analysis for whole roots. I am also grateful to Doctor Naoki Shinohara for his help on the use of dewpoint potentiometer. The support of Professor Yuko Nishimoto for conducting elemental analysis using ICP-AES were an enormous help to me.

My thanks also go to Arisa Horiuchi for her collaboration. I have had the support and encouragement of the members of Iwamoto Laboratory.

Finally, I sincerely appreciate my father, mother, and grandmother for their warm support. This thesis would not have been possible without the support of the above people, for which I am deeply grateful.